Title
MOTION OF A TWO-FLUID INTERFACE IN A POROUS MEDIUM: ANALYTICAL STUIDES

Authors
Hellstrom, G.
Tsang, C.F.
Claesson, J.

Publication Date
1986-04-01

Lawrence Berkeley Laboratory
UNIVERSITY OF CALIFORNIA

EARTH SCIENCES DIVISION

Submitted to Water Resources Research

MOTION OF A TWO-FLUID INTERFACE
IN A POROUS MEDIUM: ANALYTICAL STUDIES

G. Hellström, C-F. Tsang, and J. Claesson

April 1986

Prepared for the U.S. Department of Energy under Contract DE-AC03-76SF00098

DISCLAIMER

LBL-21313

Motion of a Two-Fluid Interface in a Porous Medium: Analytical Studies

Göran Hellström[1] and Chin-Fu Tsang

Earth Sciences Division, Lawrence Berkeley Laboratory
University of California, Berkeley, California 94720

Johan Claesson

Department of Building Technology, Lund Institute of Technology
Box 118, S-221 00, Lund, Sweden

April 1986

Submitted to Water Resources Research

[1]Also at Department of Mathematical Physics, Lund Institute of Technology, Box 118, S–221 00 Lund, Sweden.

Abstract

Analytical solutions for the pressure distribution and the flow field are derived for several idealized situations involving a vertical plane or cylindrical interface between two fluids of different density and viscosity in an infinite anisotropic aquifer bounded by two horizontal planes. The interface, or transition zone, between the two fluids may be either sharp or of finite width. The buoyancy flow induced by the density difference will cause the two-fluid interface to tilt. A characteristic time scale by which the buoyancy tilting occurs is deduced. The conditions at the well are found to have only a small influence on the buoyancy flow except very close to the well. The buoyancy flow decreases with increasing width of the transition zone. Combined buoyancy flow and forced-convection tilting are treated in detail for a straight non-vertical interface in the plane-interface case, where the tilting angle variation is given by a simple formula with only two independent parameters.

Introduction

The motion of an interface between two fluids with different densities and viscosities due to buoyancy flow and forced convection is studied. The main impetus of this study is the need to calculate the motion of the interface that occurs when fluid of one density and viscosity is injected into an aquifer stratum with fluid of another density and viscosity. The interface region constitutes a transition zone between the aquifer regions with different fluids. During an initial time period, the interface is primarily vertical. This situation is intrinsically unstable due to the difference in density between the two fluids. Buoyancy will cause the fluid of lower density to flow towards the upper part of the aquifer. The two-fluid interface will gradually tilt. Forced convection will act on the differences in viscosity, and hence in flow resistance, along different flow paths and thereby influence the tilting. Depending on the situation, the forced convection may either reinforce or counteract the pure buoyancy tilting. It is often of great interest to be able to predict the rate at which the two-fluid interface tilts.

One area of recent interest where buoyancy flow is recognized as an important phenomenon is aquifer thermal energy storage (ATES). This technology involves long-term storage of hot or chilled water mainly for space heating or cooling purposes. Research on this concept has been increasingly active during the last 10 years [*Lawrence Berkeley Laboratory*, 1978; *Tsang et al.*, 1980; *Swedish Council for Building Research*, 1983]. Theoretical studies [*Sauty et al.*, 1982a; *Doughty et al.*, 1983; *Chen and Reddell*, 1983] as well as field experiments [*Iris*, 1979; *Molz et al.*, 1979, 1981, 1983; *Sauty et al.*, 1982b] and numerical simulations thereof [*Tsang et al.*, 1981] have been completed. Strong buoyancy effects can cause a substantial reduction of the recovery factor for an ATES system [*Mathey*, 1977; *Molz et al.*, 1981]. This may require active measures, such as specific well configurations, unconventional well designs, or elaborate injection/extraction schemes, in order to prevent the detrimental effects of buoyancy

flow [*Molz et al.*, 1983; *Buscheck et al.*, 1983].

To focus our discussions, the material presented here is discussed in terms of thermally induced density and viscosity differences between the two fluids and the motion of a thermal front. However, the theory also applies to general two-fluid interface motion where density and viscosity differences occur, if capacitive effects of the solid matrix are properly accounted for. Examples of such occurrences are salt-water intrusion in a fresh-water aquifer, contaminated fluid moving in an uncontaminated aquifer, and water flooding in a petroleum reservoir.

Thermohydraulic equations

The coupled groundwater and heat flow process in the aquifer stratum is governed by two partial differential equations. The volumetric ground water flow $\overline{q}$ is related to the pressure gradient and the gravity force through the empirical law of Darcy:

$$\overline{q} = -\frac{k}{\mu}(\nabla P + \rho g \hat{z}) \tag{1}$$

The intrinsic permeability is k. The water density ρ and the viscosity μ are temperature dependent.

Equation (1) assumes isotropic permeability in the aquifer. In this paper we will also consider cases where the aquifer has different permeabilities in the horizontal (x, y) and the vertical (z) directions. The permeabilities in the horizontal and the vertical direction are denoted k and k', respectively. Then we have:

$$q_x = -\frac{k}{\mu}\frac{\partial P}{\partial x} \qquad q_y = -\frac{k}{\mu}\frac{\partial P}{\partial y} \qquad q_z = -\frac{k'}{\mu}(\frac{\partial P}{\partial z} + \rho g) \tag{2}$$

Compressibility effects are neglected, and the divergence of the groundwater flow $\overline{q}$ is then zero at each point:

$$\nabla \cdot \overline{q} = \nabla \cdot \left[-\frac{k}{\mu}(\nabla P + \rho g \hat{z}) \right] = 0 \tag{3}$$

The aquifer temperature satisfies the equation for convective-diffusive heat transfer:

$$C \frac{\partial T}{\partial t} = \nabla \cdot (\lambda \nabla T - T C_w \overline{q}) \tag{4}$$

where C and C_w are the volumetric heat capacities for the aquifer (matrix plus water) and water, respectively. The thermal conductivity is denoted λ.

The convective heat flow is given by $TC_w \overline{q}$. The thermal velocity is

$$\overline{v}_T = \frac{C_w}{C} \overline{q} \tag{5}$$

which represents the convective displacement of the temperature field.

The aquifer stratum is confined by impermeable layers at which the perpendicular ground water flow component vanishes. The temperature of injected water is given.

We will first discuss the simpler case of pure buoyancy flow and then the case of combined forced and natural convection.

Buoyancy flow

A non-uniform temperature field in the aquifer gives a variable fluid density and an ensuing buoyancy flow in the aquifer. We will in particular consider the situation when the aquifer may be divided into a warm region ($T = T_1$) and a cold region ($T = T_0$).

These regions are separated by a thermal front zone, through which the temperature falls from T_1 to T_0. The idealization of an infinitely thin or sharp thermal front will also be considered. This is often quite a useful approximation.

Let Γ be any closed curve in an isotropic aquifer ($k'=k$). The line integral along Γ of the pressure gradient is automatically zero. Darcy's relation (1) then gives:

$$\int_\Gamma \frac{\mu}{k}\,\overline{q}\cdot d\overline{r} = -g\hat{z}\cdot\int_\Gamma \rho\, d\overline{r} \tag{6}$$

The right-hand term represents a net driving force due to density variations along Γ. The left-hand side gives an integral of the tangential component of the flow $\overline{q}$ along Γ. The flow is weighted with the flow resistance coefficient μ/k. The right-hand side is known when the temperature and hence the density field is given. Equation (6) provides some information on the magnitude of the flow velocities.

Figure 1 shows a case when the curve Γ crosses a sharp thermal front. The density and the viscosity on the warm and cold sides are denoted ρ_1, μ_1 and ρ_0, μ_0 respectively. The vertical distance between the two points where Γ crosses the thermal front is H. It follows from (6) that

$$\int_{\Gamma_1} \frac{\mu_1}{k}\,\overline{q}\cdot d\overline{r} + \int_{\Gamma_0} \frac{\mu_0}{k}\,\overline{q}\cdot d\overline{r} = (\rho_0-\rho_1)\,gH \tag{7}$$

Let L_Γ denote the arc length of Γ, and q_Γ a suitable mean tangential component of $\overline{q}$ along Γ. Equation (7) may then be written:

$$q_\Gamma = \frac{k\,(\rho_0-\rho_1)g}{\mu_0+\mu_1}\cdot\frac{2H}{L_\Gamma} \tag{8}$$

The first factor will appear often in the following. We will call it the characteristic buoyancy flow q_0:

$$q_0 = \frac{k\,(\rho_0-\rho_1)g}{\mu_0+\mu_1} \tag{9}$$

Analytical solutions

Based on equations (1-3), it is possible to derive explicit expressions for the pressure distribution and the buoyancy flow pattern in some idealized situations. Figures 2a-h show the eight cases, A-H, explained in detail below. The permeability may be different in the horizontal (k) and the vertical (k') directions in all cases except in case H. We will use the notation $\kappa = \sqrt{k'/k}$.

Case A is a sharp, vertical thermal front in an infinite aquifer bounded by two impermeable horizontal planes. The thickness of the aquifer stratum is H. A vertical cross-section through the aquifer becomes an infinite strip. The expressions for the pressure distribution and the flow field are derived in Appendix A. The flow field is shown in Figure 3. A solution of a limited version of this problem for two fluids with different density, but equal viscosity ($\mu_0=\mu_1$) and isotropic permeability ($k'=k$) has previously been given by *de Josselin de Jong* [1960]. *Verruijt* [1980] solved the problem with different viscosity of the two fluids in an isotropic porous medium.

The cross-section of the aquifer stratum is a semi-infinite strip in case B and C. There is a sharp, vertical thermal front. The warmer region to the left has a horizontal thickness L. The left boundary is impermeable in case B. In case C the hydrostatic pressure $P=-\rho_1 gz$ prevails along the left, vertical boundary.

Case D and case E consider an infinite aquifer with cylindrical symmetry bounded by two horizontal planes. The warmer region occupies a cylindrical volume with radius L. There is no flow horizontal flow at the inner boundary in case D. In case E there is hydrostatic pressure $P=-\rho_1 gz$ at the inner boundary at radius $r=R_w$.

In case F we have, as in case A, an infinite aquifer bounded by two horizontal planes. The thermal front has a thickness D. The viscosity in this case is assumed to be constant, i.e. $\mu=\mu_0=\mu_1$. The density is ρ_1 in the warm region and ρ_0 in the cold region. The density is assumed to increase linearly through the thermal front region. In general, the thermal-front diffuseness D is time dependent and may be related to thermal conductivity λ by

$$D = \sqrt{\frac{16}{\pi}} \cdot \sqrt{\frac{4\lambda t}{C}} \qquad (10)$$

For our calculation of pressure distribution and buoyancy flow for a given time, a typical time t has to be chosen, and D is then proportional to $\sqrt{\lambda}$.

Case G is similar to case D with cylindrical symmetry and no horizontal flow at the inner boundary, but with a diffuse thermal front of thickness D. The viscosity is constant, i.e. $\mu=\mu_0=\mu_1$, and the density varies logarithmically through the thermal front region.

In case H the aquifer is an infinite circular cylinder. A vertical cut perpendicular to the cylinder axis becomes a circular disk with radius R (cf. Figure 2h). The permeability must be isotropic ($\kappa=1$) in this case.

The analytical solutions for these cases are derived in Appendices A-H. The given expressions are only valid at the moment when the thermal front is vertical.

The motion of the thermal front is determined by the magnitude of groundwater flow across the front. Let z denote the vertical coordinate, and let $z=0$ be at the midpoint of the aquifer. The horizontal groundwater flow across the front is denoted $q_f(z)$. The following expressions are obtained for the considered cases:

A. Infinite strip.

$$q_f(z) = \kappa q_0 \cdot \frac{1}{\pi} \ln \left[\frac{1+\sin(\frac{\pi z}{H})}{1-\sin(\frac{\pi z}{H})} \right] \tag{11}$$

B. Semi-infinite strip. Impermeable left boundary.

$$q_f(z) = \kappa q_0 \cdot \frac{4}{\pi} \sum_{n=0}^{\infty} \frac{(-1)^n}{2n+1} \cdot \frac{\sin\left[\frac{(2n+1)\pi z}{H}\right]}{\frac{\mu_0}{\mu_0+\mu_1} + \frac{\mu_1}{\mu_0+\mu_1} \coth\left[\frac{(2n+1)\pi\kappa L}{H}\right]} \tag{12}$$

C. Semi-infinite strip. Hydrostatic pressure conditions at the left boundary.

$$q_f(z) = \kappa q_0 \cdot \frac{4}{\pi} \sum_{n=0}^{\infty} \frac{(-1)^n}{2n+1} \cdot \frac{\sin\left[\frac{(2n+1)\pi z}{H}\right]}{\frac{\mu_0}{\mu_0+\mu_1} + \frac{\mu_1}{\mu_0+\mu_1} \tanh\left[\frac{(2n+1)\pi\kappa L}{H}\right]} \tag{13}$$

D. Cylindrical case. No horizontal flow at inner boundary.

$$q_f(z) = \kappa q_0 \cdot \frac{4}{\pi} \sum_{n=0}^{\infty} \frac{(-1)^n}{2n+1} \cdot \frac{\sin\left[\frac{(2n+1)\pi z}{H}\right]}{\frac{\mu_1}{\mu_0+\mu_1} \cdot \frac{I_0(\theta_n)}{I_1(\theta_n)} + \frac{\mu_0}{\mu_0+\mu_1} \cdot \frac{K_0(\theta_n)}{K_1(\theta_n)}} \tag{14}$$

where

$$\theta_n = \frac{(2n+1)\pi\kappa L}{H} \tag{15}$$

Here we have used the modified Bessel functions K_n and I_n.

E. Cylindrical case. Hydrostatic pressure conditions at inner boundary.

$$q_f(z) = \kappa q_0 \cdot \frac{4}{\pi} \sum_{n=0}^{\infty} \frac{(-1)^n}{2n+1} \cdot \sin\left[\frac{(2n+1)\pi z}{H}\right] \times \frac{1 + \frac{K_1(\theta_n^L)}{I_1(\theta_n^L)} \cdot \frac{I_0(\theta_n^R)}{K_0(\theta_n^R)}}{\frac{\mu_0-\mu_1}{\mu_0+\mu_1} \cdot \frac{K_0(\theta_n^L)}{I_1(\theta_n^L)} \cdot \frac{I_0(\theta_n^R)}{K_0(\theta_n^R)} + \frac{\mu_1}{\mu_0+\mu_1} \cdot \frac{I_0(\theta_n^L)}{I_1(\theta_n^L)} + \frac{\mu_0}{\mu_0+\mu_1} \cdot \frac{K_0(\theta_n^L)}{K_1(\theta_n^L)}} \tag{16}$$

where

$$\theta_n^R = \frac{(2n+1)\pi\kappa R_w}{H} \tag{17}$$

$$\theta_n^L = \frac{(2n+1)\pi\kappa L}{H} \tag{18}$$

F. Infinite strip with diffuse thermal front.

$$q_f(z) = \kappa q_0 \cdot \frac{4}{\pi} \sum_{n=0}^{\infty} \frac{(-1)^n}{2n+1} \cdot \frac{1 - e^{-\frac{(2n+1)\pi\kappa\frac{D}{2}}{H}}}{\frac{(2n+1)\pi\kappa\frac{D}{2}}{H}} \cdot \sin\left[\frac{(2n+1)\pi z}{H}\right] \tag{19}$$

where

$$D = \sqrt{\frac{16}{\pi}} \cdot \sqrt{\frac{4\lambda t}{C}} \tag{10}$$

The flow $q_f(z)$ refers to the middle of the thermal front region. For large values of $\kappa D/H$ equation (19) becomes:

$$q_f(z) \approx 2q_0 \cdot \frac{z}{D} \tag{20}$$

G. Cylindrical case with diffuse thermal front.

$$q_f(z) = \kappa q_0 \cdot \frac{2}{\ln\left[\frac{(L+D/2)}{(L-D/2)}\right]} \cdot \frac{4}{\pi}\sum_{n=0}^{\infty}\frac{(-1)^n}{2n+1} \cdot \left[\Phi(\theta_n^0)\frac{I_1(\theta_n^0)}{I_0(\theta_n^0)} - \right. \tag{21}$$

$$\left. \Phi(\theta_n^+)\frac{I_1(\theta_n^0)}{I_0(\theta_n^+)} + \Phi(\theta_n^0)\frac{K_1(\theta_n^0)}{K_0(\theta_n^0)} - \Phi(\theta_n^-)\frac{K_1(\theta_n^0)}{K_0(\theta_n^-)}\right] \cdot \sin\left[\frac{(2n+1)\pi z}{H}\right]$$

where the function Φ is defined by:

$$\Phi(\theta_n) = \frac{1}{\theta_n} \cdot \frac{1}{\frac{I_1(\theta_n)}{I_0(\theta_n)} + \frac{K_1(\theta_n)}{K_0(\theta_n)}} \tag{22}$$

and

$$\theta_n^+ = \frac{(2n+1)\pi\kappa(L+D/2)}{H} \tag{23}$$

$$\theta_n^0 = \frac{(2n+1)\pi\kappa L}{H} \tag{24}$$

$$\theta_n^- = \frac{(2n+1)\pi\kappa(L-D/2)}{H} \tag{25}$$

The flow $q_f(z)$ refers to the middle of the thermal front region ($r = L$).

H. Circular disk.

$$q_f(z) = q_0 \cdot \frac{1}{\pi}\left\{\left[1+\left(\frac{R}{z}\right)^2\right] \cdot \ln\left(\frac{1+\frac{z}{R}}{1-\frac{z}{R}}\right) - 2\cdot\frac{R}{z}\right\} \tag{26}$$

The flows $q_f(z)$ are all odd functions of z. Figures 4-14 show the dimensionless buoyancy flow $q_f(z)/(\kappa q_0)$, $0 \le z \le H/2$, for the different cases. The quotient between the different viscosities $\beta = \mu_0/\mu_1$ is an important parameter. In these figures, we will use

two values for β, which correspond to the following temperatures:

$$T_1=90\ ^\circ\mathrm{C} \qquad T_0=5\ ^\circ\mathrm{C} \quad \rightarrow \quad \beta=\frac{\mu_0}{\mu_1}=4.82 \tag{27}$$

$$T_1=90\ ^\circ\mathrm{C} \qquad T_0=40\ ^\circ\mathrm{C} \quad \rightarrow \quad \beta=\frac{\mu_0}{\mu_1}=2.09$$

Values for $\beta=1$ ($\mu_0=\mu_1$) are also given.

Figure 4 shows the buoyancy flow across a vertical, sharp thermal front for an infinite strip, case A. This curve is also shown in Figures 5-9 and Figure 13 for comparison. The buoyancy flow is somewhat lower when the aquifer is limited to the circular disc of case H (Figure 4). In cases B and C, the left region with temperature T_1 has a width of L. The buoyancy flow across the thermal front does not differ much from the infinite case A when $\kappa L/H$ is greater than about 0.3 (Figures 5-8). The buoyancy flow of the cylindrical cases D and E has the same character as that of the plane cases B and C, except that it is more sensitive to small values of $\kappa L/H$ (cf. Figures 5 and 9, Figures 6 and 10, Figures 7 and 11, Figures 8 and 12). The infinite strip, case A, is evidently a good approximation for the buoyancy flow across the thermal front except for thin regions with different temperature.

Figure 13 shows the buoyancy flow for a vertical thermal front region with a thickness D in an infinite aquifer. The deviation from case A with a sharp front is again rather small, when $\kappa D/H$ is less than say 0.3. The flow increases linearly with z for large $\kappa D/H$ in accordance with equation (20).

The buoyancy flow for the cylindrical case with a diffuse thermal front, case G, depends on two independent parameters $\kappa L/H$ and $\kappa D/H$. Figure 14 shows the buoyancy flow for $\kappa L/H=1$. As in case F, the flow increases linearly with z for large

$\kappa D / H$.

Tilting of a thermal front

The buoyancy flow will cause a thermal front to tilt. A quantitative measure of the rate of tilting is of great interest. For the case when there is no forced convection, the tilting rate may be defined as follows.

Consider a straight, vertical thermal front at a time t. The total water flow across the upper half of the thermal front is called the tilting flow. The same amount passes in the other direction through the lower half of the front. The tilting flow Q_t is defined by:

$$Q_t = \int_0^{H/2} q_f(z)\, dz = -\int_{-H/2}^{0} q_f(z)\, dz \tag{28}$$

Figure 15 illustrates the tilting of a vertical front. Each point on the front is displaced a length $\overline{v}_T\, dt$ during a small time increment. The displacement in the normal direction of the front is $v_{Tn} \cdot dt$, where v_{Tn} is the thermal velocity component perpendicular to the thermal front. The curved thermal front (Figure 15b) is approximated by an appropriate straight line (Figure 15c). The front is tilted an angle $\omega_t\, dt$ during the time increment dt. A heat balance for the thermal front gives:

$$\frac{1}{2} \cdot \frac{H}{2} \cdot \frac{H}{2} \tan(\omega_t\, dt) = \frac{C_w}{C}\, Q_t\, dt \tag{29}$$

The time increment is small so $\tan(\omega_t\, dt) = \omega_t\, dt$. The tilting rate then becomes:

$$\omega_t = \frac{8}{H^2} \cdot \frac{C_w}{C}\, Q_t \tag{30}$$

The tilting flow Q_t is obtained by integrating $q_f\,(z)$ over the interval $0 \leq z \leq H/2$. The integration of each term in the different series of equations (11-14, 16, 19, 21, 26) is straightforward.

The tilting flow for case A is found to be:

$$Q_t = \frac{4G}{\pi^2}\,\kappa q_0 H \qquad (G = 0.915\ldots. \text{ Catalan's constant}) \tag{31}$$

The corresponding rate of angular tilting is:

$$\omega_0 = \frac{32G}{\pi^2} \cdot \kappa \cdot \frac{C_w\, q_0}{C} \cdot \frac{1}{H} \qquad \left(\frac{32G}{\pi^2} \approx 3.0\right) \tag{32}$$

The corresponding tilting time t_0 is then:

$$t_0 = \frac{1}{\omega_0} = \frac{HC}{\kappa C_w\, k} \cdot \frac{\pi^2(\mu_0+\mu_1)}{32G\,(\rho_0-\rho_1)g} \tag{33}$$

The second factor on the right hand side is a function only of the temperatures T_0 and T_1.

In case H, the circular disk, it is possible to obtain an analytical solution for the case when the straight thermal front is tilted an angle α from the vertical direction. See Appendix H. The tilting flow and the tilting rate in case H become:

$$Q_t = \frac{2}{\pi}\, q_0\, R \cdot \cos(\alpha) \qquad \omega_t = \frac{8}{\pi} \cdot \frac{C_w\, q_0}{C} \cdot \frac{1}{2R} \cdot \frac{1}{\cos(\alpha)} \qquad \left(\frac{8}{\pi} \approx 2.5\right) \tag{34}$$

The tilting rate is thus reduced in the proportion 2.5/3.0, when an infinite strip (case A with κ=1) is compared to a corresponding circular disk with a vertical thermal front.

The tilting rate ω_t/ω_0 is shown in Figures 16-18 for β=4.82, 2.09, and 1.0 respectively for the cases A-F and H. Figure 19 shows case G. The deviation from the tilting rate ω_0 of the infinite strip is small, when $\kappa L/H$ is greater than about 0.5. The

diffuseness of the thermal front reduces the tilting flow with about 50% when $\kappa D/H = 1$.

Superposition of buoyancy and forced convection

In general, tilting in an aquifer is a combination of buoyancy flow and forced-convection tilting. The pure buoyancy flow is due to the density variations of the fluid. The other part, the forced-convection tilting, is not influenced by the density variations, but is due to viscosity variations when forced convection is present. Let P_b and P_{fc} be the two contributions to the total pressure:

$$P = P_b + P_{fc} \tag{35}$$

Let P_b be the solution of:

$$\nabla \cdot \left[\frac{\kappa}{\mu} \cdot (\nabla P_b + \rho g \hat{z}) \right] = 0 \tag{36}$$

then

$$\nabla \cdot \left[\frac{\kappa}{\mu} \nabla P_{fc} \right] = 0 \tag{37}$$

The equations (36) and (37) are for simplicity written for the isotropic case, but can be easily generalized for the anisotropic case as shown below.

The two equations (36) and (37) have different characters. Equation (37) for P_{fc} is linear. The pressure P_{fc} and the corresponding forced-convection flow are proportional to the flow rate at the injection/extraction well. Equation (36) for P_b has a source term from the variable density. The pressure P_b and the corresponding buoyancy flow are proportional to the driving density difference $\rho_0 - \rho_1$ between the two regions.

The situation shown in Figure 20 is of particular interest. A sharp, straight thermal front is tilted an angle α in an infinite aquifer bounded by two horizontal planes. Water at a flow rate of Q_1 ($m^3H_2O/s,m$) is injected through the aquifer from left to right. The volumetric groundwater flow $\overline{q}$ has two components:

$$\overline{q} = \overline{q}_b + \overline{q}_{fc} \tag{38}$$

The forced-convection part $\overline{q}_{fc}$ is the solution of (37). The flow is constant and horizontal in the undisturbed regions far away from the front to the right and to the left ($\overline{q}_{fc} \rightarrow Q_1/H \cdot \hat{x}$). The buoyancy part $\overline{q}_b$ is the solution of (36). It becomes zero far away from the front.

We may express the different parts of the groundwater flow in terms of the dimensionless parameters x/H, z/H, the tilting angle α, the viscosity ratio β, and the anisotropy factor κ. Thus we write:

$$\overline{q}_b = q_0 \cdot \overline{q}' \left(\frac{x}{H}, \frac{z}{H}, \alpha, \beta, \kappa\right) \tag{39}$$

$$\overline{q}_{fc} = \frac{Q_1}{H} \cdot \overline{q}'' \left(\frac{x}{H}, \frac{z}{H}, \alpha, \beta, \kappa\right) \tag{40}$$

The flows $\overline{q}'$ and $\overline{q}''$ are dimensionless. It can be shown in a straightforward but lengthy way that they depend on only the five given parameters.

Let $d\alpha$ be the change of tilting angle during a time increment dt. Consider the triangular area between thermal front and the vertical cut in Figure 20. This area increases when the tilting angle changes from α to $\alpha+d\alpha$. Heat balance gives:

$$\frac{1}{2} \cdot \frac{H}{2} \cdot \frac{H}{2} \left[\tan(\alpha+d\alpha) - \tan(\alpha)\right] \cdot C\,(T_1 - T_0) = C_w\,(T_1 - T_0) Q_t\,dt \tag{41}$$

or

$$\frac{d}{dt}\left[\tan(\alpha)\right] = \frac{8 C_w}{H^2 C} \cdot Q_t \tag{42}$$

The tilting flow Q_t defined by (28) for the pure buoyancy flow case will now be generalized to include forced convection and a non-vertical front. Let s, $-H/2 \leq s \leq H/2$, be a coordinate along the straight front. The tilting flow Q_t is defined by:

$$Q_t = \int_0^{H/2} q_n(s)ds - \frac{1}{2}\frac{Q_1}{H} = -\int_{-H/2}^{0} q_n(s)ds + \frac{1}{2}\frac{Q_1}{H} \tag{43}$$

where q_n is the flow normal to the front and Q_1/H is the mean flow through the aquifer. (For pure buoyancy flow and a vertical front $Q_1=0$ and $s \rightarrow z$, and (43) reduces to (28)). In general Q_t has a component Q_{bt} from the buoyancy flow and a component Q_{ft} from the forced convection:

$$Q_t = Q_{bt} + Q_{ft} \tag{44}$$

The two components are obtained from (39) and (40) by integration over the upper (or lower) part $0 \leq z \leq H/2$ for $x=0$:

$$Q_{bt} = q_0 H \cdot f_{bt}(\alpha,\beta,\kappa) \tag{45}$$

$$Q_{ft} = Q_1 \cdot f_{ft}(\alpha,\beta,\kappa) \tag{46}$$

The two functions f_{bt} and f_{ft} depend only of the dimensionless parameters α, β, and κ.

The forced-convection tilting flow is zero for a vertical front ($\alpha=0$). We have from (31):

$$f_{bt}(0,\beta,\kappa) = \frac{4G}{\pi^2}\kappa \tag{47}$$

$$f_{ft}(0,\beta,\kappa) = 0 \tag{48}$$

The variation of tilting angle with time is given by (42-46) for the present case of a sharp, straight front in an infinite horizontal aquifer. The two functions $f_{bt}(\alpha,\beta,\kappa)$ and

$f_{ft}(\alpha,\beta,\kappa)$ are yet to be determined. In the next section it will be shown that they are related to each other by a simple formula.

Stable front solution

For a straight thermal front there exists a situation where the buoyancy tilting flow Q_{bt} and the forced-convection tilting flow Q_{ft} balance each other. In this case the total tilting flow Q_t becomes zero and the thermal front is stable.

Consider again the infinite strip with a tilted thermal front as shown in Figure 20. We assume a constant horizontal flow throughout the aquifer strip:

$$\overline{q} = \frac{Q_1}{H}\,\hat{x} \tag{49}$$

The pressure in region 1 must satisfy (cf.(2)):

$$q_x = \frac{Q_1}{H} = \frac{k}{\mu_1}\,\frac{\partial P}{\partial x} \tag{50}$$

$$q_z = 0 = \frac{k'}{\mu_1}\left(\frac{\partial P}{\partial z}+\rho_1 g\right) \tag{51}$$

The pressure is then, except for an integration constant:

$$P = -\rho_1 g z - \frac{\mu_1 Q_1}{kH}\,x \tag{52}$$

In region 0 we have in the same way:

$$P = -\rho_0 g z - \frac{\mu_0 Q_1}{kH}\,x \tag{53}$$

The thermal front is given by $x = tan(\alpha)\cdot z$, $-H/2 \leq z \leq H/2$. The normal component of the flow and the pressure must be continuous at the front. The flow is

constant. The remaining requirement of continuous pressure at the front gives with (52) and (53):

$$-\rho_1 gz - \frac{\mu_1 Q_1}{kH} \cdot \tan(\alpha)z = -\rho_0 gz - \frac{\mu_0 Q_1}{kH} \cdot \tan(\alpha)z \tag{54}$$

or with (9)

$$\tan(\alpha) = -\frac{q_0 H}{Q_1} \cdot \frac{\beta+1}{\beta-1} \tag{55}$$

We have, when (55) is satisfied, the simple horizontal flow (49).

The tilting angle of equation (55) is negative when the forced flow Q_1 is positive. Figure 21 illustrates the physical situation. The buoyancy flow rotates the front clockwise ($\rho_1 < \rho_0$). The forced convection displaces the front downstream. The viscosity is lower to the left ($\mu_1 < \mu_0$). The flow in the lower protruding warm edge is enhanced. More water flows in the lower than in the upper part. This gives a counter-clockwise rotation of the front. The buoyancy and forced-convection effects oppose each other, when the tilting angle is negative. The two effects balance each other when the angle α satisfies (55).

Equation (55) may be used to deduce a relation between the two tilting functions f_{bt} and f_{ft} of equations (45) and (46). Consider a certain case when, except for Q_1, all variables α, β, κ, and q_0 and so on are given. The pumping rate Q_1 is then chosen so that (55) is satisfied. The flow is then given by (49). The thermal front will be displaced downstream, but the tilting flow Q_t is zero. We have with (45) and (46):

$$Q_t = q_0 H \cdot f_{bt}(\alpha,\beta,\kappa) + (-)\frac{q_0 H}{\tan(\alpha)} \cdot \frac{\beta+1}{\beta-1} \cdot f_{ft}(\alpha,\beta,\kappa) = 0 \tag{56}$$

The value of Q_1 from (55) has been inserted.

From (56) we get the remarkable equation:

$$f_{bt}(\alpha,\beta,\kappa) = \frac{1}{\tan(\alpha)} \cdot \frac{\beta+1}{\beta-1} \cdot f_{ft}(\alpha,\beta,\kappa) \tag{57}$$

The formula is valid for any values of α, β, and κ, although $Q_t = 0$ only when (55) is satisfied.

The function f_{ft} has to be computed with a numerical model. The buoyancy flow function f_{bt} is then obtained from (57).

Effect of anisotropic permeability

The vertical permeability k' may differ from the horizontal permeability k, as shown in (2). However, it is possible to transform an anisotropic case to an isotropic one.

We start with an anisotropic case with the permeabilities k and k'. We have the coordinates x, y, and z, the pressure distribution P and the flow $\overline{q} = (q_x, q_y, q_z)$. In order to obtain an equivalent isotropic case, the horizontal coordinates are multiplied by the anisotropy factor $\kappa = \sqrt{k'/k}$, namely

$$x' = \kappa x \qquad y' = \kappa y \qquad z' = z \tag{58}$$

where x', y', and z' are the coordinates in the isotropic case.

Let us consider a groundwater flow problem in the old and new coordinates. The pressure at corresponding points is unchanged. The flow in the horizontal plane is divided by the factor κ, while the vertical flow is divided by κ^2:

$$P'(x',y',z') = P(x,y,z) \tag{59}$$

$$q'_x = \frac{1}{\kappa} q_x \qquad q'_y = \frac{1}{\kappa} q_y \qquad q'_z = \frac{1}{\kappa^2} q_z$$

The new flow $\overline{q}'$ and pressure P' satisfy Darcy's law (2) and the mass conservation equation (3).

We will apply this result for the case with a sharp thermal front in an infinite aquifer bounded by two horizontal planes. The front is tilted an angle α in the anisotropic case. The transformation (58) to the isotropic case requires that the horizontal coordinate be multiplied by a factor κ. The tilting angle then changes to a new value α' according to

$$\tan(\alpha') = \kappa \tan(\alpha) \tag{60}$$

Let us first treat the pure buoyancy tilting (Q_1=0). The tilting flow for the anisotropic case is from (45):

$$Q_{bt} = q_0 H \cdot f_{bt}(\alpha,\beta,\kappa) \tag{61}$$

The boundary conditions are that the normal flow is zero at $z = \pm H/2$ and that the flow vanishes far away from the thermal front. These boundary conditions are directly fulfilled in the transformed problem. The tilting flow is then:

$$Q_{bt}' = q_0 H \cdot f_{bt}(\alpha',\beta,1) \tag{62}$$

According to (59) we also have that the horizontal flow is divided by κ:

$$Q_{bt}' = \frac{1}{\kappa} Q_{bt} \tag{63}$$

From (61-63) we obtain the important relation:

$$f_{bt}(\alpha,\beta,\kappa) = \kappa \, f_{bt}(\alpha',\beta,1) \tag{64}$$

From (57), (60), and (64) we get in a similar way for the forced convection:

$$f_{ft}(\alpha,\beta,\kappa) = f_{ft}(\alpha',\beta,1) \tag{65}$$

The factor κ does not appear in this case.

The two functions $f_{ft}(\alpha,\beta,\kappa)$ and $f_{bt}(\alpha,\beta,\kappa)$ have now been reduced to one unknown function $f_{ft}(\alpha',\beta,1)$. The two remaining independent variables are the tilting angle α' and the viscosity ratio β. The function $f_{ft}(\alpha',\beta,1)$ is treated in the following section.

Forced-convection tilting

The partial differential equation for the pressure P_{fc} for the forced convection component is given by (37). Equation (65) implies that we need to consider only a case with isotropic permeability (κ=1). Figure 20 shows an infinite aquifer strip with a sharp, tilted thermal front. There is a constant horizontal flow Q_1/H in the undisturbed aquifer far away from the thermal front.

The tilting flow Q_{ft} is defined by (43). The forced-convection tilting function is from (46):

$$f_{ft}(\alpha',\beta,1) = Q_{ft}/Q_1 \tag{66}$$

The function f_{ft} is zero for a vertical front (48). The derivative of f_{ft} with respect to α' is obtained by differentiating (57). For α'=0 we get with the use of (47):

$$\frac{\partial f_{ft}(\alpha',\beta,1)}{\partial \alpha'} = \frac{4G}{\pi^2} \cdot \frac{\beta-1}{\beta+1} \qquad \alpha'=0 \tag{67}$$

The limiting case with a horizontal front (α'= 90°) is simple. The flows in the upper part and the lower halves are inversely proportional to the viscosities. It follows with the use of (43) and (66) that:

$$f_{fl}(90°,\beta,\kappa) = \frac{1}{2} \cdot \frac{\beta-1}{\beta+1} \tag{68}$$

In order to evaluate f_{fl} for tilting angles between 0° and 90°, the pressure distribution P_{fc} and the flow pattern have been computed numerically with the use of a finite difference model. Figure 22 shows an example of the flow pattern. The tilting angle of the thermal front is α'. The viscosity is lower in the warm region to left ($\mu_1 < \mu_0$), which for this case implies lower flow resistance for forced convection in the upper part of the aquifer. Therefore, the flow becomes stronger in the upper half, and the thermal front will tilt.

The numerical calculations have been performed for two viscosity ratios according to (27). The calculations were made for several angles α'. Table 1 shows the result.

The tilting rate formulas in the following section will contain the quantity:

$$\frac{\pi^2}{4G} \cdot \frac{1}{\tan(\alpha')} \cdot \frac{\beta+1}{\beta-1} \cdot f_{fl}(\alpha',\beta,1) \tag{69}$$

This expression is plotted in Figure 23 from the values of Table 1 with $s = \tan(\alpha')$ as independent variable. The points for the two values of β lie very close to each other. It is reasonable to approximate equation (69) with a single curve. We have with good accuracy:

$$\frac{\pi^2}{4G} \cdot \frac{1}{\tan(\alpha')} \cdot \frac{\beta+1}{\beta-1} \cdot f_{fl}(\alpha',\beta,1) = f_t(\tan(\alpha')) \tag{70}$$

We will call $f_t(s)$ the basic tilting function. It is shown in Figure 23.

From the basic tilting function we get with (70), (65), (60), and (57) the two tilting functions $f_{fl}(\alpha,\beta,\kappa)$ and $f_{bl}(\alpha,\beta,\kappa)$:

$$f_{bl}(\alpha,\beta,\kappa) = \frac{4G}{\pi^2} \cdot \kappa \cdot f_t(\kappa\tan(\alpha)) \tag{71}$$

$$f_{ft}(\alpha,\beta,\kappa) = \frac{4G}{\pi^2} \cdot \kappa\tan(\alpha) \cdot \frac{\beta-1}{\beta+1} \cdot f_t(\kappa\tan(\alpha)) \tag{72}$$

The value $f_t(0)$ is obtained from the derivative of (70) with respect to α' at the point $\alpha'=0$. We have with (67):

$$f_t(0) = 1 \tag{73}$$

The asymptotic value of $f_t(s)$ for large s is from (68) and (70) of the form $\pi^2/(8Gs)$. The dashed curve in Figure 23 shows this asymptote. The function $f_t(s)$ is linear in the interval $0 \leq s \leq 2$. We have with good accuracy:

$$f_t(s) \approx 1-f_1 \cdot s \qquad 0 \leq s \leq 2 \qquad f_1=0.235 \tag{74}$$

The function $f_t(s)$ is given in Table 2.

Tilting rate formula

A relatively simple formula for the tilting rate of a sharp thermal front in an infinite aquifer strip will be presented in this section. See Figure 20. The tilting angle is a function of time: $\alpha=\alpha(t)$. The aquifer may exhibit a vertical anisotropy ($\kappa \neq 1$). The value of the forced-convection flow Q_1 may be positive, zero, or negative. The combined effect of buoyancy and forced convection is considered.

The equation for the change of the tilting angle is given by (42). The tilting flow is obtained from (43-46). The two tilting functions $f_{bt}(\alpha,\beta,\kappa)$ and $f_{ft}(\alpha,\beta,\kappa)$ are given by (71) and (72) respectively. Finally we get by the use of the basic tilting function $f_t(s)$, and the basic tilting time t_0 (33) the following equation for $\alpha(t)$:

$$\frac{d}{dt}(\tan(\alpha)) = \frac{1}{t_0} f_t(\kappa\tan(\alpha)) \cdot \left[1+\frac{Q_1}{q_0 H} \cdot \frac{\beta-1}{\beta+1} \tan(\alpha)\right] \tag{75}$$

Let us use the variable

$$s = \kappa \tan(\alpha) \tag{76}$$

We also introduce the parameter:

$$\gamma = \frac{Q_1}{\kappa q_0 H} \cdot \frac{\beta-1}{\beta+1} \tag{77}$$

The quantity γ is a measure of the forced-convection flow Q_1/H compared to the characteristic buoyancy flow q_0. An alternative expression for γ may be given if (9) is used:

$$\gamma = \frac{Q_1}{\kappa k g H} \cdot \frac{\mu_0-\mu_1}{\rho_0-\rho_1} \tag{78}$$

Using the characteristic tilting time (33), we have:

$$\gamma = \frac{32G}{\pi^2} \cdot \frac{\beta-1}{\beta+1} \cdot \frac{C_w Q_1 t_0}{CH^2} \tag{79}$$

The last factor of (79) has the following physical interpretation. The horizontal volumetric flow is Q_1/H. The corresponding thermal velocity (5) is $C_w Q_1/(CH)$. The thermal front is displaced a distance $C_w Q_1 t_0/(CH)$ during the characteristic tilting time. The last factor of (79) is therefore the quotient of this displacement and the thickness of the aquifer stratum.

We may write (75) in the following way:

$$\frac{ds}{dt} = \frac{\kappa}{t_0} \cdot f_t(s)(1+\gamma s) \tag{80}$$

The basic tilting function $f_t(s)$ is given by Figure 23 and Table 2. The tilting $s = \kappa \tan(\alpha)$ is function of the dimensionless time $\kappa t / t_0$. There is only one parameter γ.

In order to solve equation (80) it is rewritten in the following way:

$$\frac{ds}{f_t(s)(1+\gamma s)} = \frac{\kappa}{t_0}dt \tag{81}$$

We introduce the following integral:

$$S(s,\gamma) = \int_0^s \frac{ds'}{f_t(s')(1+\gamma s')} \tag{82}$$

The variable s is positive: $0 \leq s < \infty$. The parameter γ may assume any value: $-\infty < \gamma < \infty$. For negative γ the integrand becomes infinite when $s' = 1/\gamma$. The integral is infinite for $s = -1/\gamma$. We get one curve for $0 \leq s < -1/\gamma$ and another for $-1/\gamma < s < \infty$. See Figure 24.

We can use approximation (74) when $0 \leq s \leq 2$. The integration of (82) is then elementary. We get:

$$S(s,\gamma) = \frac{1}{\gamma + f_1} \cdot \ln\left(\frac{|1+\gamma s|}{1-f_1 s}\right) \qquad (f_1 \doteq 0.235) \qquad 0 \leq s \leq 2 \tag{83}$$

Expression (83) is not defined when $\gamma = -f_1$. Then we have by direct integration:

$$S(s,-f_1) = \frac{s}{1-f_1} \tag{84}$$

The function $S(s,\gamma)$ is shown in Figure 24.

The solution of (80) during a period with constant γ is with (81-82) given by:

$$S(s_2,\gamma) - S(s_1,\gamma) = \frac{\kappa(t_2 - t_1)}{t_0} \qquad s_2 = s(t_2) \qquad s_1 = s(t_1) \tag{85}$$

The tilting $s = \kappa \tan\alpha$ will follow the curves of Figures 24. As an example of application, Figure 25 illustrates what happens during a storage cycle. We have an injection period with $\gamma = 1$. Then there is a storage period with $\gamma = 0$. During the extraction

period we take γ=–1. Figure 25 shows the three curves $S(s,\gamma)$ from Figure 24. We start at t =0 with a vertical front: s =0, and follow the curve $S(s,1)$ for a time interval t corresponding to the duration of the injection period. The tilting s at the end of the injection period becomes s_1. During the ensuing rest period the tilting follows the curve $S(s,0)$ from $s=s_1$ to $s=s_2$. The curve $S(s,-1)$ is followed during the extraction period to a final tilting s_3.

Figure 26 illustrates what may happen if the durations of the injection, storage, and extraction periods are increased. The three curves $S(s,1)$, $S(s,0)$, and $S(s,-1)$ are again shown from Figure 24. The extraction curve $S(s,-1)$ has two branches. The tilting s_2 after the injection and the storage periods is greater than s =1. Therefore, the tilting proceeds along the upper branch of $S(s,-1)$.

The tilting s moves toward the asymptotic value -1/γ during the extraction phase for the case when $T_{-}>T_0$. The upper decreasing branch is followed, when the initial tilting s_2 is greater than $-1/\gamma$. For a case with cold water injection and extraction, $T_1<T_0$, the asymptotic value is approached during the injection period. At the asymptotic limit we have with the use of (76):

$$s = \kappa\tan(\alpha) = \frac{-1}{\gamma} = \frac{\kappa q_0 H}{-Q_1}\cdot\frac{\beta+1}{\beta-1} \tag{86}$$

This is precisely the condition (55) for a stable front. The flow is horizontal and constant throughout the aquifer (49).

We will end this section with an explicit formula for the tilting angle $\alpha(t)$. We assume that $0\leq s\leq 2$, $s=\kappa\tan(\alpha)$, so that (80) is valid. Our case concerns a period with pure buoyancy flow (γ=0) or injection with a positive γ-value. The thermal front is initially vertical:

$$\gamma \geq 0 \qquad \alpha(0) = 0 \tag{87}$$

From (76), (83) and (85) we get:

$$\tan(\alpha(t)) = \frac{1}{\kappa} \cdot \frac{1-e^{-(\gamma+f_1)\kappa t/t_0}}{f_1+\gamma e^{-(\gamma+f_1)\kappa t/t_0}} \qquad (\kappa\tan(\alpha) < 2) \tag{88}$$

Relation between motions of a thermal interface and a solute-concentration interface.

The tilting of a two-fluid interface has been discussed in terms of thermally induced density and viscosity differences between hot and cold fluids and the motion of a thermal front. The theory also applies to general two-fluid interface motion where density and viscosity differences occur. The relation between the case involving heat transport and that involving solute transport will be discussed below.

Capacitive effects of the solid matrix in the aquifer will cause the two-fluid interface to move at a lower velocity than individual fluid particles. The mechanism by which the capacitive effects occur is different for heat and solute transport. For heat transport, the capacitive effects are due to the heating up of the solid matrix of the porous medium and are accounted for by the factor C/C_w in the equations presented in this paper (cf. equation (5)). In the case of solute transport, the solute may react with or be adsorbed onto the solid matrix and we have to use another factor, which will be derived in the following paragraphs.

Let v be the groundwater velocity and v_T the velocity of the two-fluid interface. A retardation factor R_s may be defined for the case when the flow is approximately one-dimensional [*Davis and DeWiest*, 1966; *Javandel et al.*, 1984]:

$$R_s = \frac{v}{v_T} \tag{89}$$

The retardation factor for solute transport may also be written [*Grove*, 1976]:

$$R_s = \left(1+\frac{\rho_b K_d}{n}\right) \tag{90}$$

Here, ρ_b denotes the bulk density of the solid matrix, K_d is a measure of solute adsorption capacity of the medium, called the distribution coefficient, and n is the effective porosity of the porous medium. Values of K_d have been measured in the laboratory and in the field [*Patterson and Spoel*, 1981; *Pickens et al.*, 1981].

The velocity of a thermal front is given by equation (5). The fluid velocity is $|\,\overline{q}\,|/n$. The retardation factor for heat transport then becomes:

$$R_s = \frac{1}{n}\,\frac{C}{C_w} \tag{91}$$

The formulas given in this paper for the motion of the thermal front can be applied to a two-fluid interface during solute transport if the retardation factors (90) and (91) are equal, i.e. if we set

$$\frac{C}{C_w} = nR_s \tag{92}$$

where R_s is given by equation (90).

In the case of a conservative, i.e. non-reactive, solute, $K_d = 0$ and $R_s = 1$. Then C/C_w should be set to n.

For the case of solute transport, an additional phenomenon needs to be considered. This is the well-known and much studied dispersion tensor, which takes into account the inhomogeneity of the porous medium. Recent work by *Güven et al.*, [1985], based on an analysis of field data, indicates that if one takes into account in detail the vertical

permeability distribution of the aquifer, the remaining dispersive effect will be very small -- on the order of that of laboratory samples. For one-dimensional flow, there is an equivalence relation [*Sauty*, 1982a] between thermal conductivity λ and dispersivity d given by

$$\lambda = dC_w \overline{q} \tag{93}$$

Thus if one-dimensional flow across the two-fluid interface is a good approximation, then the results of cases F and G in this paper are applicable by substituting for λ in equations (19) through (25) according to equation (93). If this approximation is not valid, then one would have to introduce the dispersion term into the governing equation (4) and redevelop the complete theory.

Summary and conclusions

The present paper describes the results of a detailed study of the motion of a two-fluid interface, where the two fluids have different densities and viscosities. While the equations and solutions are presented in terms of a thermal interface, discussions are given to show how they are applicable to other kinds of fluids with different solute concentrations and other physical properties.

The basic equations for the thermohydraulic process in the aquifer are given by (2), (3), and (4). The groundwater flow in the aquifer with its displacement and, in particular, its tilting of the thermal front may be considered as a superposition of a buoyancy flow and a forced-convection flow. The buoyancy flow is at work all the time, while the forced convection takes place during periods of injection and extraction.

First the pure buoyancy flow of a vertical front is analyzed. The starting point of the analysis is a series of exact solutions for the groundwater flow for various geometries shown in Figures 2a-h. The flow across the thermal front determines the tilting rate of the front. The most important case is the sharp front in an infinite aquifer bounded by two horizontal planes. This case gives the tilting rate with good accuracy except for quite thin warm regions ($\kappa L / H < 0.3$) and for quite thick thermal fronts ($\kappa D / H > 0.3$).

The superposition of buoyancy and forced convection is defined by equations (35-37). A detailed analysis is made for the case with a sharp, tilted thermal front in an infinite aquifer bounded by two horizontal planes (Figure 20). The tilting flow Q_t may be written (43-46):

$$Q_t = q_0 H \cdot f_{bt}(\alpha,\beta,\kappa) + Q_1 \cdot f_{ft}(\alpha,\beta,\kappa)$$

The characteristic buoyancy flow q_0 is defined by (9). The two functions f_{bt} and f_{ft} for the buoyancy tilting and the forced-convection tilting respectively depend only on the tilting angle α, the viscosity ratio $\beta = \mu_0/\mu_1$, and the anisotropy parameter $\kappa = \sqrt{k'/k}$.

For a certain combination of tilting angle and forced-convection flow rate the total flow in the aquifer is constant and horizontal. The tilting rate is then zero (55). From this we may deduce a relation (57) between $f_{bt}(\alpha,\beta,\kappa)$ and $f_{ft}(\alpha,\beta,\kappa)$:

$$f_{bt}(\alpha,\beta,\kappa) = \frac{1}{\tan(\alpha)} \cdot \frac{\beta+1}{\beta-1} \cdot f_{ft}(\alpha,\beta,\kappa) \qquad (57)$$

The effect of anisotropic permeability is analyzed. It is possible to reduce an anisotropic case to an isotropic case by a simple coordinate transformation (58). The forced-convection tilting function (46) reduces to:

$$f_{ft}(\alpha,\beta,\kappa) = f_{ft}(\alpha',\beta,1) \qquad (65)$$

with

$$\tan(\alpha') = \kappa \tan(\alpha) \tag{60}$$

The remaining unknown function $f_{ft}(\alpha',\beta,1)$ is computed numerically. It is shown that we can express the results with a single function $f_t(s)$:

$$f_{ft}(\alpha',\beta,1) = \frac{4G}{\pi^2} \tan(\alpha') \frac{\beta-1}{\beta+1} f_t(\tan(\alpha')) \tag{70}$$

The basic tilting function $f_t(s)$, which is given in Figure 23 and Table 2, is linear in the interval $0 \leq s \leq 2$:

$$f_t(s) = 1 - f_1 \cdot s \qquad 0 \leq s \leq 2 \qquad f_1 = 0.235 \tag{74}$$

The final formula for the tilting rate of a sharp, tilted front in an infinite aquifer bounded by two horizontal planes becomes:

$$\frac{ds}{dt} = \frac{\kappa}{t_0} f_t(s)(1+\gamma s) \tag{80}$$

$$s = \kappa \tan(\alpha) \tag{76}$$

$$\gamma = \frac{Q_1}{\kappa q_0 H} \cdot \frac{\beta-1}{\beta+1} \tag{77}$$

The solution of (80) is simple for $0 \leq s \leq 2$ when (74) is valid. The tilting s will follow the curves in Figure 24. Two examples of the tilting angle variation $\alpha(t)$ during a storage cycle are given by Figures 25 and 26.

Some specific observations and conclusions are summarized below:

1. The buoyancy tilting flow is induced by a density difference between the fluids, whereas the forced-convection also induces a tilting flow because of a difference in

viscosity.

2. The two basic parameters for the tilting rate of the thermal front are the characteristic tilting time t_0 and the forced-convection tilting parameter γ given by equations (33) and (77) respectively.

3. The buoyancy tilting rate (32) is inversely proportional to the height H of the aquifer.

4. The tilting rate is proportional to an effective permeability that equals $\sqrt{k'k}$, where k is the horizontal permeability and k' is the vertical permeability.

5. For fluid of one temperature, T_1, injected into an aquifer of another temperature, T_0, the tilting rate depends on the temperatures, since the density, and particularly the viscosity, exhibit a strong temperature dependence.

6. Let L denote the distance from the well to the vertical thermal front. The influence on the buoyancy tilting from the boundary of the well is negligible if $\kappa L / H > 0.5$. This applies both to the plane and the cylindrical case.

7. The diffuseness of the thermal front diminishes the tilting rate. Let D be an appropriate width of the front. The tilting rate is reduced by 50%, when D increases from $D = 0$ to $\kappa D / H = 1$.

8. During forced convection there exists a situation (55) where the front is stable, i.e. with no tilting flow. This situation occurs during extraction of hot water which was stored in a cold aquifer, or during injection of cold water into a warm aquifer.

Nomenclature

C aquifer volumetric heat capacity (matrix plus water), J/m^{3}K.

C_w volumetric heat capacity of water, J/m^{3}K.

d dispersivity, m.

D thickness of diffuse thermal front in cases F and G, m.

f_{bt} buoyancy tilting function.

f_{ft} forced-convection tilting function.

f_t basic tilting function.

f_1 =0.235

g standard gravity, 9.81 m/s^2.

G Catalan's constant (=0.915...).

H thickness of aquifer stratum, m.

k permeability (horizontal), m^2.

k' vertical permeability, m^2.

L horizontal thickness of region left of the thermal front in case B, C, D, E, and G, m.

n effective porosity of porous medium.

P pressure, Pa.

P_b pressure for buoyancy flow part of equation (35), Pa.

P_{fc} pressure for forced convection part of equation (35), Pa.

$\overline{q}$ volumetric groundwater flux, m^{3}H$_2$O/m^{2}s.

$\overline{q}_b$ volumetric groundwater flux for buoyancy flow part of equation (35), m^{3}H$_2$O/m^{2}s.

$\overline{q}_{fc}$ volumetric groundwater flux for forced convection part of equation (35), m^{3}H$_2$O/m^{2}s.

q_x x-component of $\overline{q}$, m^{3}H$_2$O/m^{2}s.

q_y y-component of $\overline{q}$, m^3H_2O/m^2s.

q_z z-component of $\overline{q}$, m^3H_2O/m^2s.

q_f horizontal buoyancy flow across thermal front, m^3H_2O/m^2s.

q_0 characteristic buoyancy flow defined by equation (9), m^3H_2O/m^2s.

Q_t tilting flow, m^3H_2O/s.

Q_{bt} buoyancy tilting flow, m^3H_2O/s.

Q_{ft} forced-convection tilting flow, m^3H_2O/s.

Q_1 forced-convection flow rate through aquifer, m^3H_2O/s.

r radial coordinate, m.

R radius of circular region in case H, m.

R_s retardation factor for solute transport.

R_w radius at inner boundary in case E, m.

s tilting parameter equal to $\kappa\tan\alpha$.

S tilting function defined by equation (82).

t time, s.

t_0 characteristic tilting time defined by equation (33), s.

T temperature, °C.

T_0 temperature of region 0, °C.

T_1 temperature of region 1, °C.

$\overline{v}_T$ thermal velocity equal to $C_w\,\overline{q}\,/C$, m/s.

x horizontal coordinate, m.

y horizontal coordinate, m.

z vertical coordinate, m.

α tilting angle. Angle between straight thermal front and vertical axis.

α' tilting angle for isotropic case ($\kappa=1$).

β viscosity factor, equal to μ_0/μ_1.

γ forced-convection tilting parameter defined by equation (77).

κ anisotropy factor, equal to $\sqrt{k'/k}$.

λ thermal conductivity, W/mK.

μ dynamic viscosity, kg/ms.

μ_0 dynamic viscosity in region 0, kg/ms.

μ_1 dynamic viscosity in region 1, kg/ms.

ρ density, kg/m^3.

ρ_0 density in region 0, kg/m^3.

ρ_1 density in region 1, kg/m^3.

ω_t angular tilting rate defined by equation (30), rad/s.

ω_0 angular tilting rate for case A, given by equation (32), rad/s.

Acknowledgements

This work was supported by the Director, Office of Energy Research, Office of Basic Energy Science, Division of Engineering, Mathematics, and Geosciences and also the U.S. Department of Energy under contract No. DE-AC03-76SF00098. On the Swedish side, the work has been supported by the Swedish Council for Building Research (BFR) and the National Swedish Board for Energy Source Development (NE)

The authors also wish to express their gratitude to Dr. Bengt Aberg at Department of Hydraulics, Royal Institute of Technology, Stockholm, Sweden, and Christine Doughty at Earth Sciences Division, Lawrence Berkeley Laboratory, Berkeley, for stimulating discussions and good suggestions.

References

Buscheck, T.A., C. Doughty, and C.F. Tsang, Prediction and analysis of a field experiment on a multi-layered aquifer thermal energy storage system with strong buoyancy flow, *Water Resour. Res., 19(5)*, 1307-1316, 1983.

Chen, C.S., and D.L. Reddell, Temperature distribution around a well during thermal injection and a graphical technique for evaluating aquifer thermal properties, *Water Resour. Res., 19(2),* 351-363, 1983.

Davis, S.N., and R.J.M. DeWiest, *Hydrogeology,* 463 pp., John Wiley, New York, 1966.

de Josselin de Jong, G., Singularity distributions for the analysis of multiple-fluid flow through porous media, *J. Geophys. Res., 65,* 3739-3758, 1960.

Doughty, C., G. Hellström, C. F. Tsang, and J. Claesson, A dimensionless parameter approach to the thermal behavior of an aquifer thermal energy storage system, *Water Resour. Res., 18(3),* 571-587, 1982.

Güven, R., R.W. Falta, F.J. Molz, and J.G. Melville, Analysis and interpretation of single-well tracer tests in stratified aquifers, *Water Resour. Res., 21(5)* ,676-684, 1985.

Grove, D.B., Ion exchange reactions important in groundwater quality models, in *Advances in Groundwater Hydrology*: Proceedings of a Symposium, Chicago, Ill., pp. 144-152, American Water Res. Assoc., Minneapolis, Minn., 1976.

Javandel, I., C. Doughty, and C.F. Tsang, *Groundwater Transport: Handbook of Mathematical Models,* 228 pp., Water Resources Monograph, Vol. 10, American Geophysical Union, Washington D.C., 1984.

Lawrence Berkeley Laboratory, Proceedings of Thermal Energy Storage in Aquifers Workshop, *Rep. LBL-8491,* Berkeley, Calif., 1978.

Mathey, B., Development and resorption of a thermal disturbance in a phreatic aquifer with natural convection, *J. Hydrol., 34,* 315-333, 1977.

Molz, F.J., A.D. Parr, P.F. Andersen, V.D. Lucido, and J.C. Warman, Thermal energy storage in a confined aquifer: Experimental results, *Water Resour. Res., 15(6),* 1506-1514, 1979.

Molz, F.J., A.D. Parr, and P.F. Andersen, Thermal energy storage in a confined aquifer: Second cycle, *Water Resour. Res., 17(3),* 611-615, 1981.

Molz, F.J., J.G. Melville, A.D. Parr, D.A. King, and M.T. Hopf, Aquifer thermal energy

storage: A well doublet experiment at increased temperatures, *Water Resour. Res., 19(1)*, 149-160, 1983.

Patterson, R.J., and T. Spoel, Laboratory measurements of the Strontium distribution coefficent K_d^{Sr} for sediments from a shallow sand aquifer, *Water Resour. Res., 17(3)*, 513-520, 1981.

Pickens, J.F., R.E. Jackson, K.J. Inch, and W.F. Merrit, Measurement of distribution coefficents using a radial injection dual-tracer test, *Water Resour. Res., 17(3)*, 529-544, 1981.

Sauty, J.P., A.C. Gringarten, A. Menjoz, and P.A. Landel, Sensible energy storage in aquifers, 1, Theoretical study, *Water Resour. Res., 18(2)*, 245-252, 1982a.

Sauty, J.P., A.C. Gringarten, H. Fabris, D. Thiery, A. Menjoz, and P.A. Landel, Sensible energy storage in aquifers, 2, Field experiments and comparison with theoretical results, *Water Resour. Res., 18(2)*, 253-265, 1982b.

Swedish Council for Building Research, Proc. of Int. Conf. on Subsurface Heat Storage, *BFR-Document D16:1983*, Stockholm, Sweden, 1983.

Tsang, C.F., D. Hopkins, and G. Hellström, Aquifer thermal energy storage - A survey, *Rep. LBL-10441*, Lawrence Berkeley Lab., Berkeley, Calif., 1980.

Tsang, C.F., T.A. Buscheck, and C. Doughty, Aquifer thermal energy storage: A numerical simulation of Auburn University field experiments, *Water Resour. Res., 17(3)*, 647-658, 1981.

Verruijt, A., The rotation of a vertical interface in a porous medium, *Water Resour. Res., 16(1)*, 239-240, 1980.

TABLE 1. The Function $f_{fl}(\alpha',\beta,1)$ as a Function of the Tilting Angle α' and the Viscosity Ratio β for the Isotropic Case (κ=1).

	Tilting angle α'						
$\beta=\mu_0/\mu_1$	0°	15°	30°	45°	60°	75°	90°
2.09	0.000	0.033	0.067	0.099	0.131	0.158	0.176
4.82	0.000	0.061	0.125	0.189	0.251	0.302	0.328

TABLE 2. The Basic Tilting Function $f_t(s)$.

	Tilting parameter $s = \kappa\tan(\alpha)$						
	0	0.268	0.577	1.000	1.732	3.732	∞
$\alpha'(\kappa=1)$†	0°	15°	30°	45°	60°	75°	90°
$f_t(s)$	1	0.937	0.864	0.765	0.593	0.329	0

† The tilting angle α' corresponding to a certain value of s is given for the isotropic case ($\kappa=1$).

Appendix A. Analytical Solution for a Sharp, Vertical Thermal Front in an Infinite Strip.

An analytical expression for the pressure distribution in case A, which is shown in Figure 2a, will be derived in this appendix. The aquifer stratum occupies the region $-\infty < x < \infty, -H/2 < z < H/2$. The thermal front is located at $x=0$, $-H/2 < z < H/2$.

Let $P(x,z)$ denote the pressure distribution in the aquifer. In region 1, $x < 0, -H/2 < z < H/2$, the pressure satisfies:

$$\frac{\partial}{\partial x}\left(\frac{k}{\mu_1}\frac{\partial P}{\partial x}\right)+\frac{\partial}{\partial z}\left[\frac{k'}{\mu_1}\left(\frac{\partial P}{\partial z}+\rho_1 g\right)\right]=0 \tag{A1}$$

In region 0, $x > 0, -H/2 < z < H/2$, we have:

$$\frac{\partial}{\partial x}\left(\frac{k}{\mu_0}\frac{\partial P}{\partial x}\right)+\frac{\partial}{\partial z}\left[\frac{k'}{\mu_0}\left(\frac{\partial P}{\partial z}+\rho_0 g\right)\right]=0 \tag{A2}$$

The upper and lower boundaries are impermeable:

$$\frac{\partial P}{\partial z}+\rho_1 g = 0 \qquad z = \pm\frac{H}{2}, -\infty < x < 0 \tag{A3}$$

$$\frac{\partial P}{\partial z}+\rho_0 g = 0 \qquad z = \pm\frac{H}{2}, \quad 0 < x < \infty \tag{A4}$$

Hydrostatic conditions prevail far away from the thermal front:

$$P \rightarrow -\rho_1 g z \qquad x \rightarrow -\infty \tag{A5}$$

$$P \rightarrow -\rho_0 g z \qquad x \rightarrow +\infty \tag{A6}$$

The pressure and the groundwater flow are continuous at the thermal front:

$$P(-0,z) = P(+0,z) \qquad -\frac{H}{2} < z < \frac{H}{2} \tag{A7}$$

$$-\frac{k}{\mu_1}\cdot\frac{\partial P}{\partial x}=-\frac{k}{\mu_0}\cdot\frac{\partial P}{\partial x} \qquad x=0, -\frac{H}{2} < z < \frac{H}{2} \tag{A8}$$

We start with the following expressions:

$$x<0: \quad P(x,z) = -\rho_1 g z + \sum_{n=0}^{\infty} a_n u_n(x,z) \tag{A9}$$

$$x>0: \quad P(x,z) = -\rho_0 g z + \sum_{n=0}^{\infty} b_n u_n(x,z) \tag{A10}$$

where

$$u_n(x,z) = \sin\left[\frac{(2n+1)\pi z}{H}\right] \cdot e^{-\frac{(2n+1)\pi\kappa\,|\,x\,|}{H}} \tag{A11}$$

It is not difficult to verify that these expressions satisfy (A1-A6) for any choice of the coefficients a_n and b_n. The coefficients are determined by the two remaining conditions (A7) and (A8):

$$a_n = -\frac{q_0 H \mu_1}{k} \cdot \frac{4}{\pi^2} \cdot \frac{(-1)^n}{(2n+1)^2} \tag{A12}$$

$$b_n = -\frac{\mu_0}{\mu_1} \cdot a_n \tag{A13}$$

In particular we have for the flow across the thermal front:

$$q_f(z) = -\frac{k}{\mu_1} \cdot \frac{\partial P}{\partial x} = \kappa q_0 \cdot \frac{4}{\pi} \sum_{n=0}^{\infty} \frac{(-1)^n}{2n+1} \cdot \sin\left[\frac{(2n+1)\pi z}{H}\right] \tag{A14}$$

The series may be expressed in the simpler form of equation (11).

Appendix B. Analytical Solution for a Sharp, Vertical Thermal Front in a Semi-Infinite Strip; Impermeable Left Boundary.

An analytical expression for the pressure distribution in case B, which is shown in Figure 2b, will be derived in this appendix. The aquifer stratum occupies the region $0 < x < \infty$, $-H/2 < z < H/2$. The thermal front is located at $x = L$, $-H/2 < z < H/2$.

Let $P(x,z)$ denote the pressure distribution in the aquifer. In region 1, $0 < x < L$, $-H/2 < z < H/2$, the pressure satisfies equation (A1). In region 0, $x > L$, $-H/2 < z < H/2$, we have equation (A2).

The upper and lower boundaries are impermeable:

$$\frac{\partial P}{\partial z}+\rho_1 g = 0 \qquad z=\pm\frac{H}{2},\ 0 < x < L \tag{B1}$$

$$\frac{\partial P}{\partial z}+\rho_0 g = 0 \qquad z=\pm\frac{H}{2},\ L < x < \infty \tag{B2}$$

Hydrostatic conditions far away from the thermal front give (A6). The left boundary is impermeable:

$$\frac{\partial P}{\partial x} = 0 \qquad x=0,\ -\frac{H}{2} < z < \frac{H}{2} \tag{B3}$$

The pressure and the groundwater flow are continuous at the thermal front:

$$P(-L,z) = P(+L,z) \qquad -\frac{H}{2} < z < \frac{H}{2} \tag{B4}$$

$$-\frac{k}{\mu_1}\cdot\frac{\partial P}{\partial x}=-\frac{k}{\mu_0}\cdot\frac{\partial P}{\partial x} \qquad x=L,\ -\frac{H}{2} < z < \frac{H}{2} \tag{B5}$$

We start with the following expressions:

$$0<x<L: \qquad P(x,z) = -\rho_1 g z + \sum_{n=0}^{\infty} a_n \sin\left[\frac{(2n+1)\pi z}{H}\right]\cdot\cosh\left[\frac{(2n+1)\pi\kappa x}{H}\right] \tag{B6}$$

$$x>L: \qquad P(x,z) = -\rho_0 g z + \sum_{n=0}^{\infty} b_n \sin\left[\frac{(2n+1)\pi z}{H}\right]\cdot e^{-\frac{(2n+1)\pi\kappa(x-L)}{H}} \tag{B7}$$

These expressions satisfy (A1-A2), (B1-B3), and (A6) for any choice of the coefficients a_n and b_n: The coefficients are determined by the two remaining conditions (B4) and (B5).

$$a_n = -\frac{q_0 H \mu_1}{k}\cdot\frac{1}{\frac{\mu_0}{\mu_0+\mu_1}\sinh(\theta_n)+\frac{\mu_1}{\mu_0+\mu_1}\cosh(\theta_n)}\cdot\frac{4}{\pi^2}\frac{(-1)^n}{(2n+1)^2} \tag{B8}$$

$$\bar{b}_n = -\frac{\mu_0}{\mu_1} \cdot \sinh(\theta_n) \cdot a_n \tag{B9}$$

where

$$\theta_n = \frac{(2n+1)\pi\kappa L}{H} \tag{B10}$$

Finally we obtain the flow across the thermal front (12) by differentiation of (B6) or (B7).

Appendix C. Analytical Solution for a Sharp, Vertical Thermal Front in a Semi-Infinite Strip; Hydrostatic Pressure Conditions at the Left Boundary.

An analytical expression for the pressure distribution in case C, which is shown in Figure 2c, will be derived in this appendix. The aquifer stratum occupies the region $0 < x < \infty, -H/2 < z < H/2$. The thermal front is located at $x = L$, $-H/2 < z < H/2$.

Let $P(x,z)$ denote the pressure distribution in the aquifer. In region 1, where $0 < x < L$, $-H/2 < z < H/2$, the pressure satisfies equation (A1). In region 0, where $x > L$, $-H/2 < z < H/2$, we have equation (A2).

The upper and lower boundaries are impermeable, which implies the boundary conditions (B1-B2). Hydrostatic conditions far away from the thermal front give (A6). Hydrostatic conditions prevail at the left boundary:

$$P(0,z) = -\rho_1 g z \qquad -\frac{H}{2} < z < \frac{H}{2} \tag{C1}$$

The pressure and the groundwater flow are continuous at the thermal front as expressed by (B4) and (B5). We start with (B7) for $x > L$ and the following expression for $0 < x < L$:

$$P(x,z) = -\rho_1 g z + \sum_{n=0}^{\infty} a_n \sin\left[\frac{(2n+1)\pi z}{H}\right] \cdot \sinh\left[\frac{(2n+1)\pi\kappa x}{H}\right] \tag{C2}$$

Expressions (C2) and (B7) satisfy (A1-A2), (B1-B2), (C1), and (A6) for any choice of the coefficients a_n and b_n : the coefficients are determined by the two remaining conditions (B4) and (B5).

$$a_n = -\frac{q_0 H \mu_1}{k} \cdot \frac{1}{\frac{\mu_0}{\mu_0+\mu_1}\cosh(\theta_n)+\frac{\mu_1}{\mu_0+\mu_1}\sinh(\theta_n)} \cdot \frac{4}{\pi^2}\frac{(-1)^n}{(2n+1)^2} \tag{C3}$$

$$b_n = -\frac{\mu_0}{\mu_1} \cdot \cosh(\theta_n) \cdot a_n \tag{C4}$$

where θ_n is defined by (B10).

The flow across the thermal front (13) is obtained by differentiation of (C2) or (B7) with a_n and b_n given by (C3) and (C4) respectively.

Appendix D. Analytical Solution for a Sharp, Vertical Thermal Front in the Cylindrical Case; No Flow at the Inner Boundary.

An analytical expression for the pressure distribution in case D, which is shown in Figure 2d, will be derived in this appendix. Cylindrical coordinates, r and z, are used. The aquifer stratum occupies the region $0 < r < \infty$, $-H/2 < z < H/2$. The thermal front is located at $r = L$, $-H/2 < z < H/2$.

Let $P_1(r,z)$ denote the pressure distribution in region 1, $0 < r < L$, $-H/2 < z < H/2$. The pressure satisfies:

$$\frac{1}{r}\frac{\partial}{\partial r}\left(\frac{k}{\mu_1} r \frac{\partial P_1}{\partial r}\right)+\frac{\partial}{\partial z}\left[\frac{k'}{\mu_1}\left(\frac{\partial P_1}{\partial z}+rho_1 g\right)\right] = 0 \tag{D1}$$

In region 0, $r > L$, $-H/2 < z < H/2$. We have for the pressure $P_0(r,z)$:

$$\frac{1}{r}\frac{\partial}{\partial r}\left(\frac{k}{\mu_0} r \frac{\partial P_0}{\partial r}\right)+\frac{\partial}{\partial z}\left[\frac{k'}{\mu_0}\left(\frac{\partial P_0}{\partial z}+rho_0 g\right)\right] = 0 \tag{D2}$$

The upper and lower boundaries are impermeable:

$$\frac{\partial P_1}{\partial z}+\rho_1 g = 0 \qquad z = \pm \frac{H}{2}, \quad 0 < r < L \tag{D3}$$

$$\frac{\partial P_0}{\partial z}+\rho_0 g = 0 \qquad z = \pm \frac{H}{2}, \quad L < r < \infty \tag{D4}$$

At the inner boundary, $r = 0$, symmetry requires that:

$$\frac{\partial P_1}{\partial r} = 0 \qquad -\frac{H}{2} < z < \frac{H}{2} \tag{D5}$$

Hydrostatic conditions prevail far away from the thermal front:

$$P_0 \rightarrow -\rho_0 g z \qquad r \rightarrow \infty \tag{D6}$$

The pressure and the groundwater flow are continuous at the thermal front:

$$P_1(L,z) = P_0(L,z) \qquad -\frac{H}{2} < z < \frac{H}{2} \tag{D7}$$

$$-\frac{k}{\mu_1} \cdot \frac{\partial P_1}{\partial r} = -\frac{k}{\mu_0} \cdot \frac{\partial P_0}{\partial r} \qquad r = L, \; -\frac{H}{2} < z < \frac{H}{2} \tag{D8}$$

We start with the following expressions:

$$P_1(r,z) = -\rho_1 g z + \sum_{n=0}^{\infty} a_n \sin\left[\frac{(2n+1)\pi z}{H}\right] \cdot I_0\left[\frac{(2n+1)\pi \kappa r}{H}\right] \tag{D9}$$

$$P_0(r,z) = -\rho_0 g z + \sum_{n=0}^{\infty} b_n \sin\left[\frac{(2n+1)\pi z}{H}\right] \cdot K_0\left[\frac{(2n+1)\pi \kappa r}{H}\right] \tag{D10}$$

Here we make use of the modified Bessel functions I_n and K_n. These expressions satisfy (D1-D6) for any choice of the coefficients a_n and b_n. The coefficients are determined by the two remaining conditions (D7) and (D8).

$$a_n = \frac{q_0 H \mu_1}{k} \cdot \frac{1}{\frac{\mu_1}{\mu_0+\mu_1} \cdot \frac{I_0(\theta_n)}{I_1(\theta_n)} + \frac{\mu_0}{\mu_0+\mu_1} \cdot \frac{K_0(\theta_n)}{K_1(\theta_n)}} \cdot \frac{1}{I_1(\theta_n)} \cdot \frac{4}{\pi^2} \frac{(-1)^n}{(2n+1)^2} \tag{D11}$$

$$b_n = -\frac{\mu_0}{\mu_1} \frac{I_1(\theta_n)}{K_1(\theta_n)} \cdot a_n \tag{D12}$$

where θ_n is given by (B10).

Finally we obtain the flow across the thermal front (14) by differentiation of (D9) or (D10).

Appendix E. Analytical Solution for a Sharp, Vertical Thermal Front in the Cylindrical Case; Hydrostatic Pressure Conditions at the Inner Boundary.

An analytical expression for the pressure distribution in case E, which is shown in Figure 2e, will be derived in this appendix. Cylindrical coordinates, r and z, are used. The aquifer stratum occupies the region $R_w < r < \infty, -H/2 < z < H/2$. The thermal front is located at $r = L$, $-H/2 < z < H/2$.

Let $P_1(r,z)$ denote the pressure distribution in region 1, where $R_w < r < L$, $-H/2 < z < H/2$. The pressure P_1 satisfies equation (D1). For the pressure $P_0(r,z)$ in region 0, $r > L$, $-H/2 < z < H/2$, we have equation (D2).

The upper and lower boundaries are impermeable, which implies the boundary conditions (D3-D4). Hydrostatic conditions far away from the thermal front give (D6). We also have hydrostatic pressure conditions at the inner boundary, $r = R_w$:

$$P_1(R_w,z) = -\rho_1 g z \qquad -\frac{H}{2} < z < \frac{H}{2} \tag{E1}$$

Pressure and groundwater flow are continuous at the thermal front as expressed by (D7) and (D8).

We start with the following expressions:

$$P_1(r,z) = -\rho_1 g z + \sum_{n=0}^{\infty} a_n u_n(r,z) + \sum_{n=0}^{\infty} b_n v_n(r,z) \tag{E2}$$

$$P_0(r,z) = -\rho_0 g z + \sum_{n=0}^{\infty} c_n v_n(r,z) \tag{E3}$$

where

$$u_n(r,z) = \sin\left[\frac{(2n+1)\pi z}{H}\right] \cdot I_0\left[\frac{(2n+1)\pi\kappa r}{H}\right] \tag{E4}$$

$$v_n(r,z) = \sin\left[\frac{(2n+1)\pi z}{H}\right] \cdot K_0\left[\frac{(2n+1)\pi\kappa r}{H}\right] \tag{E5}$$

These expressions satisfy (D1-D4) and (D6) for any choice of the coefficients a_n, b_n, and c_n. The coefficients are determined by the three remaining conditions (E1), (D7), and (D8).

$$a_n = \frac{q_0 H \mu_1}{k} \cdot \frac{1}{I_1(\theta_n^L)} \cdot \frac{4}{\pi^2} \cdot \frac{(-1)^n}{(2n+1)^2} \times \tag{E6}$$

$$\frac{1}{\frac{\mu_0-\mu_1}{\mu_0+\mu_1} \cdot \frac{K_0(\theta_n^L)}{I_1(\theta_n^L)} \cdot \frac{I_0(\theta_n^R)}{K_0(\theta_n^R)} + \frac{\mu_1}{\mu_0+\mu_1} \cdot \frac{I_0(\theta_n^L)}{I_1(\theta_n^L)} + \frac{\mu_0}{\mu_0+\mu_1} \cdot \frac{K_0(\theta_n^L)}{K_1(\theta_n^L)}}$$

$$b_n = -\frac{I_0(\theta_n^R)}{K_0(\theta_n^R)} \cdot a_n \tag{E7}$$

$$c_n = -\frac{\mu_0}{\mu_1} \cdot \frac{I_1(\theta_n^L)}{K_1(\theta_n^L)} \cdot \left[1 + \frac{K_1(\theta_n^L)}{I_1(\theta_n^L)} \cdot \frac{I_0(\theta_n^R)}{K_0(\theta_n^R)}\right] \cdot a_n \tag{E8}$$

where

$$\theta_n^R = \frac{(2n+1)\pi\kappa R_w}{H} \tag{E9}$$

$$\theta_n^L = \frac{(2n+1)\pi\kappa L}{H} \tag{E10}$$

Finally we obtain the flow across the thermal front (16) by differentiation of (E4) or (E5).

Appendix F. Analytical Solution for an Infinite Strip with Diffuse Thermal Front.

An analytical expression for the pressure distribution in case F, which is shown in Figure 2f, will be derived in this appendix. The aquifer stratum occupies the region $-\infty < x < \infty, -H/2 < z < H/2$. The thermal front region, which has a thickness D, is located at $-D/2 < x < D/2, -H/2 < z < H/2$. The viscosity is constant in this case ($\mu=\mu_0=\mu_1$). The density is ρ_1 in region 1, where $x < -D/2, -H/2 < z < H/2$, and ρ_1 in region 0, where $x > D/2, -H/2 < z < H/2$. The density in the thermal front region varies linearly with x between ρ_1 and ρ_0:

$$\rho(x) = \frac{1}{2}(\rho_0+\rho_1)+\frac{x}{D}(\rho_0-\rho_1) \tag{F1}$$

The pressure distribution $P_1(x,z)$ in region 1 satisfies (A1) with $\mu_1=\mu$. For the pressure $P_0(x,z)$ in region 0, we have equation (A2) with $\mu_0=\mu$. The pressure $P_D(x,z)$ in the thermal front region is the solution of:

$$\frac{\partial}{\partial x}(\frac{k}{\mu}\frac{\partial P_D}{\partial x})+\frac{\partial}{\partial z}\left[\frac{k'}{\mu}(\frac{\partial P_D}{\partial z}+\rho(x)g)\right] = 0 \tag{F2}$$

The upper and lower boundaries are impermeable, so that

$$\frac{\partial P}{\partial z}+\rho g = 0 \qquad z = \pm\frac{H}{2} \tag{F3}$$

for the different regions. Hydrostatic conditions far away from the thermal front give (A5-A6).

The pressure and the groundwater flow are continuous at the interfaces between the thermal front region and the surrounding regions:

$$P_1(-D/2,z) = P_D(-D/2,z) \qquad -\frac{H}{2} < z < \frac{H}{2} \tag{F4}$$

$$P_0(D/2,z) = P_D(D/2,z) \qquad -\frac{H}{2} < z < \frac{H}{2} \tag{F5}$$

$$-\frac{k}{\mu}\cdot\frac{\partial P_1}{\partial x}=-\frac{k}{\mu}\cdot\frac{\partial P_D}{\partial x} \qquad x=-D/2,\ -\frac{H}{2}<z<\frac{H}{2} \tag{F6}$$

$$-\frac{k}{\mu}\cdot\frac{\partial P_0}{\partial x}=-\frac{k}{\mu}\cdot\frac{\partial P_D}{\partial x} \qquad x=D/2,\ -\frac{H}{2}<z<\frac{H}{2} \tag{F7}$$

We start with the following expressions:

$$P_1(x,z)=-\rho_1 gz+\sum_{n=0}^{\infty}a_n\,u_n(x,z) \tag{F8}$$

$$P_0(x,z)=-\rho_0 gz+\sum_{n=0}^{\infty}b_n\,v_n(x,z) \tag{F9}$$

$$P_D(x,z)=-\rho(x)gz+\sum_{n=0}^{\infty}c_n\,u_n(x,z)+\sum_{n=0}^{\infty}d_n\,v_n(x,z) \tag{F10}$$

where

$$u_n(x,z)=\sin\left[\frac{(2n+1)\pi z}{H}\right]\cdot e^{\frac{(2n+1)\pi\kappa x}{H}} \tag{F11}$$

$$v_n(x,z)=\sin\left[\frac{(2n+1)\pi z}{H}\right]\cdot e^{-\frac{(2n+1)\pi\kappa x}{H}} \tag{F12}$$

These expressions satisfy (A1-A2), (F2-F3), (A5-A6) for any choice of the coefficients a_n, b_n, c_n, and d_n. The coefficients are determined by the four remaining conditions (F4-F7):

$$a_n=\frac{q_0 H\mu}{2k}\cdot\frac{4}{\pi^2}\cdot\frac{(-1)^n}{(2n+1)^2}\cdot\frac{H}{(2n+1)\pi\kappa\frac{D}{2}}\left(e^{-\frac{(2n+1)\pi\kappa\frac{D}{2}}{H}}-e^{\frac{(2n+1)\pi\kappa\frac{D}{2}}{H}}\right) \tag{F13}$$

$$b_n=-a_n \tag{F14}$$

$$c_n=\cdot\frac{q_0 H\mu}{2k}\cdot\frac{4}{\pi^2}\cdot\frac{(-1)^n}{(2n+1)^2}\cdot\frac{H}{(2n+1)\pi\kappa\frac{D}{2}}\cdot e^{-\frac{(2n+1)\pi\kappa\frac{D}{2}}{H}} \tag{F15}$$

$$d_n=-c_n \tag{F16}$$

In particular we have for the flow across a vertical cut in the middle of the thermal region:

$$q_f(z) = -\frac{k}{\mu} \cdot \frac{\partial P_D}{\partial x} \qquad x=0 \tag{F17}$$

The result may be expressed as the series of equation (19).

Appendix G. Analytical Solution for the Cylindrical Case with Diffuse Thermal Front.

An analytical expression for the pressure distribution in case G, which is shown in Figure 2g, will be derived in this appendix. The aquifer stratum occupies the region $0 < r < \infty, -H/2 < z < H/2$. The thermal front region, which has a thickness D, is located at $L-D/2 < r < L+D/2$, $-H/2 < z < H/2$. The thermal front region must not extend into the well, i.e. $D < 2L$. The viscosity is constant in this case ($\mu=\mu_0=\mu_1$). The density is ρ_1 in region 1, $0 < r < L-D/2$, $-H/2 < z < H/2$, and ρ_0 in region 0, $r > L+D/2$, $-H/2 < z < H/2$. The density in the thermal front region varies with r between ρ_1 and ρ_0 according to:

$$\rho(r) = \frac{\rho_1 \ln\left[\frac{(L+D/2)}{r}\right] + \rho_0 \ln\left[\frac{r}{(L-D/2)}\right]}{\ln\left[\frac{(L+D/2)}{(L-D/2)}\right]} \tag{G1}$$

The pressure distribution $P_1(r,z)$ in region 1 satisfies (D1) with $\mu_1=\mu$. For the pressure $P_0(r,z)$ in region 0, we have equation (D2) with $\mu_0=\mu$. The pressure $P_D(r,z)$ in the thermal front region is the solution of:

$$\frac{1}{r}\frac{\partial}{\partial r}\left(\frac{k}{\mu} r \frac{\partial P_D}{\partial r}\right) + \frac{\partial}{\partial z}\left[\frac{k'}{\mu}\left(\frac{\partial P_D}{\partial z} + \rho(r) g\right)\right] = 0 \tag{G2}$$

The upper and lower boundaries are impermeable, so that

$$\frac{\partial P}{\partial z}+\rho g = 0 \qquad z = \pm\frac{H}{2} \tag{G3}$$

for the different regions. The no-horizontal-flow condition at the inner boundary, $r = 0$, and hydrostatic conditions far away from the thermal front give (D5-D6).

The pressure and the groundwater flow are continuous at the interfaces between the thermal front region and the surrounding regions:

$$P_1(L-D/2,z) = P_D(L-D/2,z) \qquad -\frac{H}{2} < z < \frac{H}{2} \tag{G4}$$

$$P_0(L+D/2,z) = P_D(L+D/2,z) \qquad -\frac{H}{2} < z < \frac{H}{2} \tag{G5}$$

$$-\frac{k}{\mu}\cdot\frac{\partial P_1}{\partial r} = -\frac{k}{\mu}\cdot\frac{\partial P_D}{\partial r} \qquad r = L-D/2,\ -\frac{H}{2} < z < \frac{H}{2} \tag{G6}$$

$$-\frac{k}{\mu}\cdot\frac{\partial P_0}{\partial r} = -\frac{k}{\mu}\cdot\frac{\partial P_D}{\partial r} \qquad r = L+D/2,\ -\frac{H}{2} < z < \frac{H}{2} \tag{G7}$$

We start with the following expressions:

$$P_1(r,z) = -\rho_1 g z + \sum_{n=0}^{\infty} a_n u_n(r,z) \tag{G8}$$

$$P_0(r,z) = -\rho_0 g z + \sum_{n=0}^{\infty} b_n v_n(r,z) \tag{G9}$$

$$P_D(r,z) = -\rho(r) g z + \sum_{n=0}^{\infty} c_n u_n(r,z) + \sum_{n=0}^{\infty} d_n v_n(r,z) \tag{G10}$$

where the functions $u_n(r,z)$ and $v_n(r,z)$ are given by (E4) and (E5) respectively.

These expressions satisfy (D1-D2), (G2-G3), (D5-D6) for any choice of the coefficients a_n, b_n, c_n, and d_n. The coefficients are determined by the four remaining conditions (G4-G7):

$$a_n = \frac{2 q_0 H \mu}{k}\cdot\frac{1}{\ln\left[\dfrac{(L+D/2)}{(L-D/2)}\right]}\cdot\frac{4}{\pi^2}\cdot\frac{(-1)^n}{(2n+1)^2}\cdot\left[\frac{\Phi(\theta_n^+)}{I_0(\theta_n^+)}-\frac{\Phi(\theta_n^-)}{I_0(\theta_n^-)}\right] \tag{G11}$$

$$b_n = \frac{2q_0 H\mu}{k} \cdot \frac{1}{\ln\left[\frac{(L+D/2)}{(L-D/2)}\right]} \cdot \frac{4}{\pi^2} \cdot \frac{(-1)^n}{(2n+1)^2} \cdot \left[\frac{\Phi(\theta_n^+)}{K_0(\theta_n^+)} - \frac{\Phi(\theta_n^-)}{K_0(\theta_n^-)}\right] \quad \text{(G12)}$$

$$c_n = \frac{2q_0 H\mu}{k} \cdot \frac{1}{\ln\left[\frac{(L+D/2)}{(L-D/2)}\right]} \cdot \frac{4}{\pi^2} \cdot \frac{(-1)^n}{(2n+1)^2} \cdot \frac{\Phi(\theta_n^+)}{I_0(\theta_n^+)} \quad \text{(G13)}$$

$$d_n = -\frac{2q_0 H\mu}{k} \cdot \frac{1}{\ln\left[\frac{(L+D/2)}{(L-D/2)}\right]} \cdot \frac{4}{\pi^2} \cdot \frac{(-1)^n}{(2n+1)^2} \cdot \frac{\Phi(\theta_n^-)}{K_0(\theta_n^-)} \quad \text{(G14)}$$

where the function Φ is defined by:

$$\Phi(\theta_n) = \frac{1}{\theta_n} \cdot \frac{1}{\frac{I_1(\theta_n)}{I_0(\theta_n)} + \frac{K_1(\theta_n)}{K_0(\theta_n)}} \quad \text{(G15)}$$

and

$$\theta_n^+ = \frac{(2n+1)\pi\kappa(L+D/2)}{H} \quad \text{(G16)}$$

$$\theta_n^- = \frac{(2n+1)\pi\kappa(L-D/2)}{H} \quad \text{(G17)}$$

In particular we have for the flow across a vertical cut in the middle of the thermal region:

$$q_f(z) = -\frac{k}{\mu} \cdot \frac{\partial P_D}{\partial r} \qquad r = L \quad \text{(G18)}$$

The result may be expressed as the series of equation (21).

Appendix H. Analytical Solution for a Sharp Thermal Front in a Circular Region.

An analytical expression for the pressure distribution in case H, which is shown in Figure 2h, will be derived in this appendix. The aquifer has the shape of an infinite

circular cylinder with an horizontal symmetry axis. A vertical cut through the cylinder becomes a circular disk with radius R. We first consider the case with a vertical thermal front. Both polar coordinates (r, ϕ) and cartesian coordinates (x, z) are used. Here ϕ denotes the angle with respect to the upward vertical direction, which is denoted $\hat{z}$. Let $P_1(r, \phi)$ denote the pressure distribution in the the left part of the circular region, $0 < r < R$, $-\pi < \phi < 0$. In the right part, $0 < r < R$, $0 < \phi < \pi$, the pressure is $P_0(r, \phi)$. The pressures P_1 and P_0 both satisfy:

$$\frac{1}{r}\frac{\partial}{\partial r}(r\frac{\partial P}{\partial r})+\frac{1}{r^2}\frac{\partial^2 P}{\partial \phi^2} = 0 \qquad \text{(H1)}$$

The periphery of the disk is impermeable. Let $\hat{r}$ and $\hat{z}$ denote unit vectors in the radial and vertical direction respectively. Then we have:

$$\frac{\partial P_1}{\partial r}+\rho_1 g\hat{z}\cdot\hat{r} = 0 \qquad r=R, -\pi < \phi < 0 \qquad \text{(H2)}$$

$$\frac{\partial P_0}{\partial r}+\rho_0 g\hat{z}\cdot\hat{r} = 0 \qquad r=R, 0 < \phi < \pi \qquad \text{(H3)}$$

The pressure and the groundwater flow are continuous at the thermal front:

$$P_1(r, \phi) = P_0(r, \phi) \qquad 0 < r < R, \phi = 0 \text{ and } \pm\pi \qquad \text{(H4)}$$

$$-\frac{k}{\mu_1}\cdot\frac{\partial P_1}{\partial x}=-\frac{k}{\mu_0}\cdot\frac{\partial P_0}{\partial x} \qquad 0 < r < R, \phi = 0 \text{ and } \pm\pi \qquad \text{(H5)}$$

where x is a horizontal coordinate.

We start with the following expressions:

$$P_1(r, \phi) = -\alpha r\cos(\phi) + \sum_{n=1}^{\infty} a_n (\frac{r}{R})^{2n} \cdot \sin(2n\phi) \qquad \text{(H6)}$$

$$P_0(r, \phi) = -\alpha r\cos(\phi) + \sum_{n=1}^{\infty} b_n (\frac{r}{R})^{2n} \cdot \sin(2n\phi) \qquad \text{(H7)}$$

These expressions satisfy (H1) for any choice of the coefficients α, a_n, and b_n. The coefficients are determined by the four remaining conditions (H2-H5):

$$\alpha = \frac{(\mu_0\rho_1 + \mu_1\rho_0)g}{\mu_0 + \mu_1} \tag{H8}$$

$$a_n = -\frac{q_0 R\,\mu_1}{k} \cdot \frac{4}{\pi} \cdot \frac{1}{(2n+1)(2n-1)} \tag{H9}$$

$$b_n = \frac{\mu_0}{\mu_1} \cdot a_n \tag{H10}$$

The pressure in the aquifer is now:

$$P_i(r,\phi) = -\frac{(\mu_0\rho_1 + \mu_1\rho_0)gz}{\mu_0+\mu_1} - \frac{q_0 R\,\mu_i}{k}\,\tilde{P}\left(\frac{r}{R},\phi\right) \tag{H11}$$

where $i=0$ for $0 < \phi < \pi$ and $i=1$ for $-\pi < \phi < 0$. We have introduced a dimensionless pressure:

$$\tilde{P}(r',\phi) = -\frac{4}{\pi}\sum_{n=1}^{\infty} \frac{1}{(2n+1)(2n-1)} \cdot (r')^{2n} \cdot \sin(2n\,\phi) \tag{H12}$$

This series may be expressed in closed form with the use of the complex number

$$w = r'\cos(\phi) + i\;r'\sin(\phi) = (z+ix)/R \tag{H13}$$

The dimensionless pressure (H12) may then be written:

$$\tilde{P} = -\frac{1}{\pi}\,\mathrm{Im}\left[\left(w-\frac{1}{w}\right) ln\left(\frac{1+w}{1-w}\right)\right] = -\frac{1}{\pi}\,\mathrm{Im}\left[\,f\,(w)\,\right] \tag{H14}$$

The symbol Im denotes the imaginary part. An evaluation of the complex function $f\,(w)$ gives:

$$\tilde{P} = -\frac{1}{\pi}\Bigg\{\left(r'-\frac{1}{r'}\right)\cos(\phi)\cdot \arctan\left[\frac{2r'\sin(\phi)}{1-(r')^2}\right] \tag{H15}$$

$$+\frac{1}{2}\left(r'+\frac{1}{r'}\right)\sin(\phi)\cdot \ln\left[\frac{1+(r')^2+2r'\cos(\phi)}{1+(r')^2-2r'\cos(\phi)}\right]\Bigg\}$$

In particular we have for the flow across the thermal front:

$$q_f(z) = -q_0 R\cdot\frac{\partial\tilde{P}}{\partial x} = \frac{q_0}{\pi}\cdot \mathrm{Re}\left[\frac{df}{dw}\right] \tag{H16}$$

Here Re denotes the real part. The result is given in equation (26).

In this particular case it is possible solve the problem with a straight thermal front which is tilted an angle α from a vertical position. By making the substitution:

$$\phi' = \phi - \alpha \tag{H17}$$

we find that equations (H1-H7) remain unchanged except that the gravitational constant g is replaced by $g \cdot \cos(\alpha)$. This means that all pressures and flows are reduced by the factor $\cos(\alpha)$ when the thermal front is tilted an angle α.

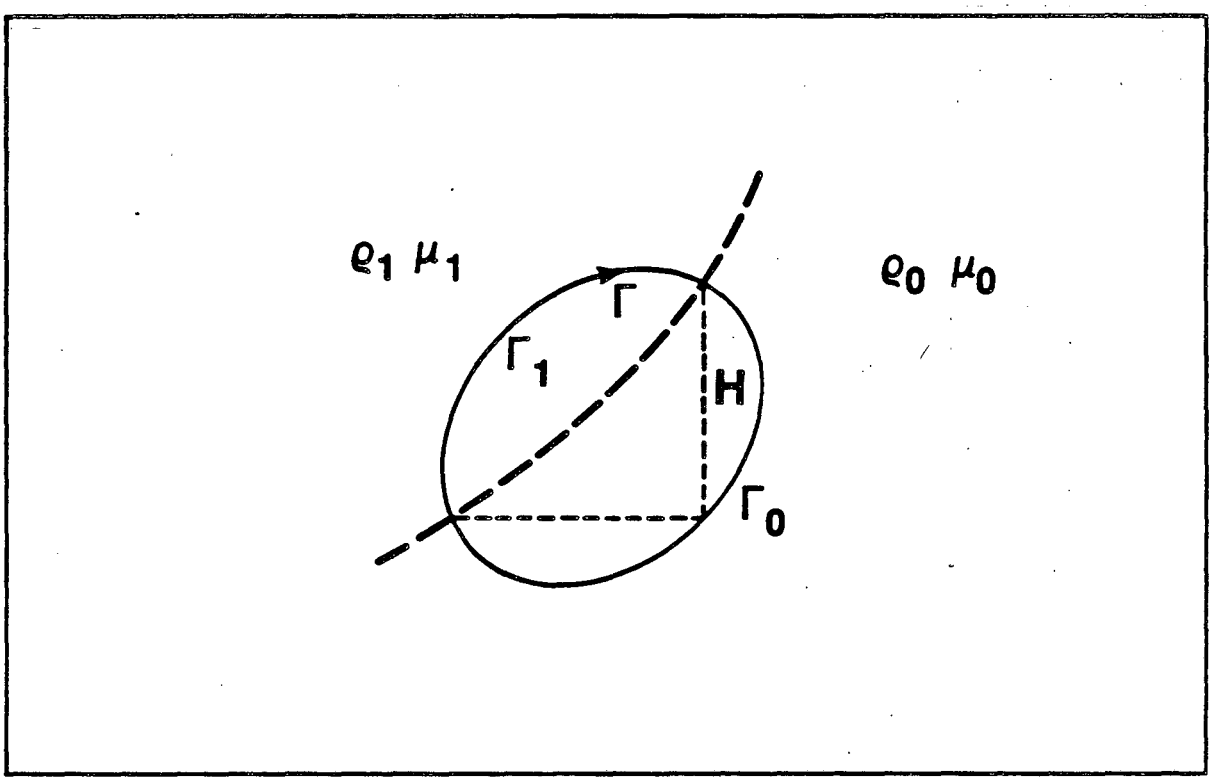

XBL 854-11027

Fig. 1. Closed curve Γ in an aquifer with a sharp thermal front (dashed line).

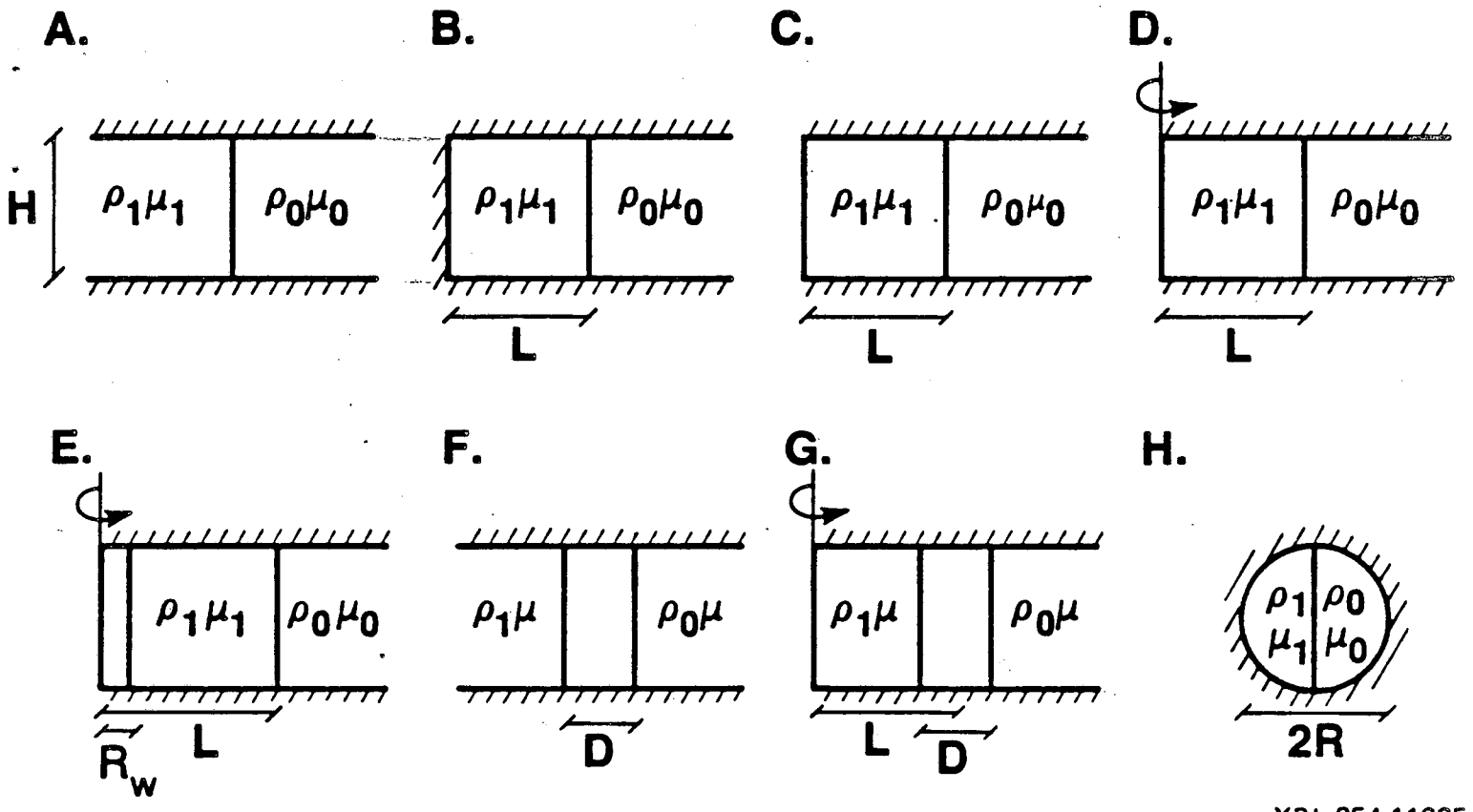

Fig. 2. Cases considered for analytical solutions: (A) Infinite strip. (B) Semi-infinite strip with impermeable left boundary. (C) Semi-infinite strip with hydrostatic conditions along the left boundary. (D) Cylindrical case with no horizontal flow at inner boundary. (E) Cylindrical case with hydrostatic pressure conditions at inner boundary. (F) Infinite strip with thermal front thickness D. (G) Cylindrical case with thermal front thickness D. (H) Circular disc.

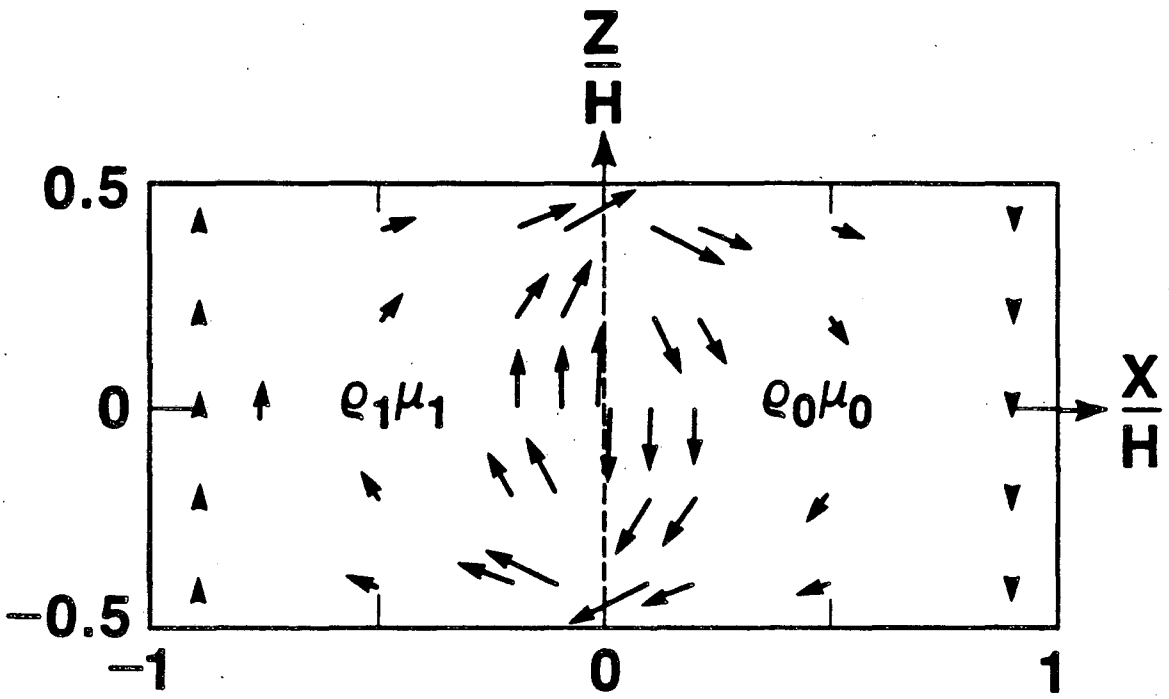

Fig. 3. Flow field $\overline{q}$ in case A (κ=1).

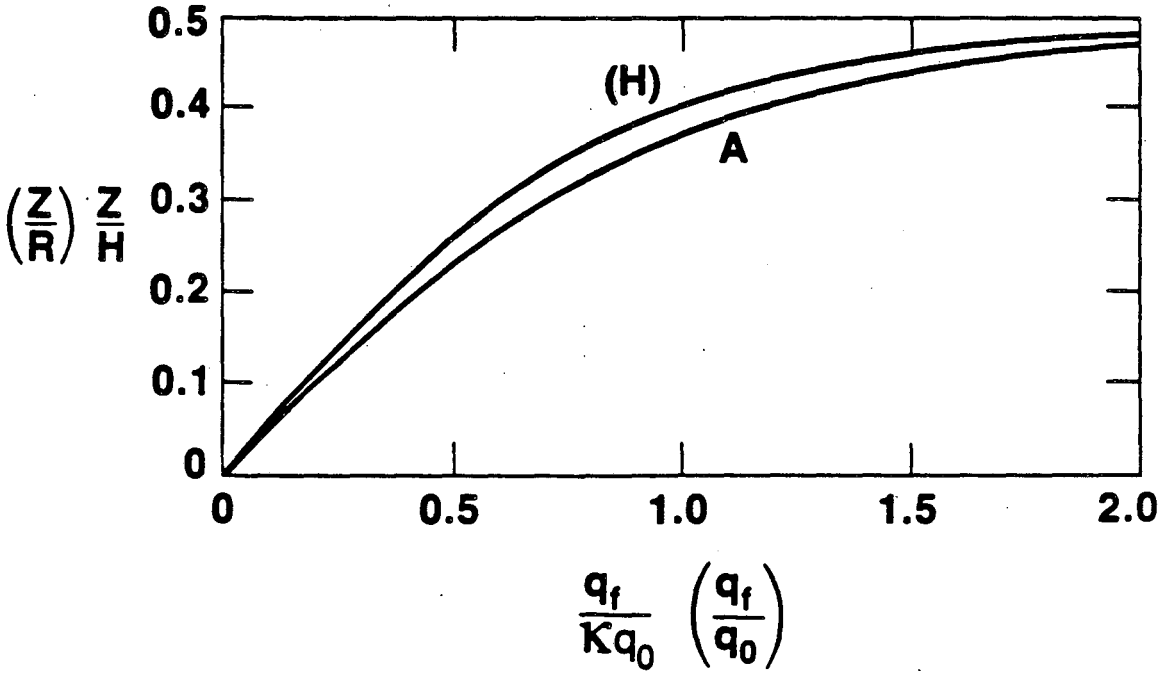

Fig. 4. Dimensionless horizontal groundwater flow across the thermal front for the infinite strip (case A) and the circular disc (case H). The parameters within parentheses concern the circular disc.

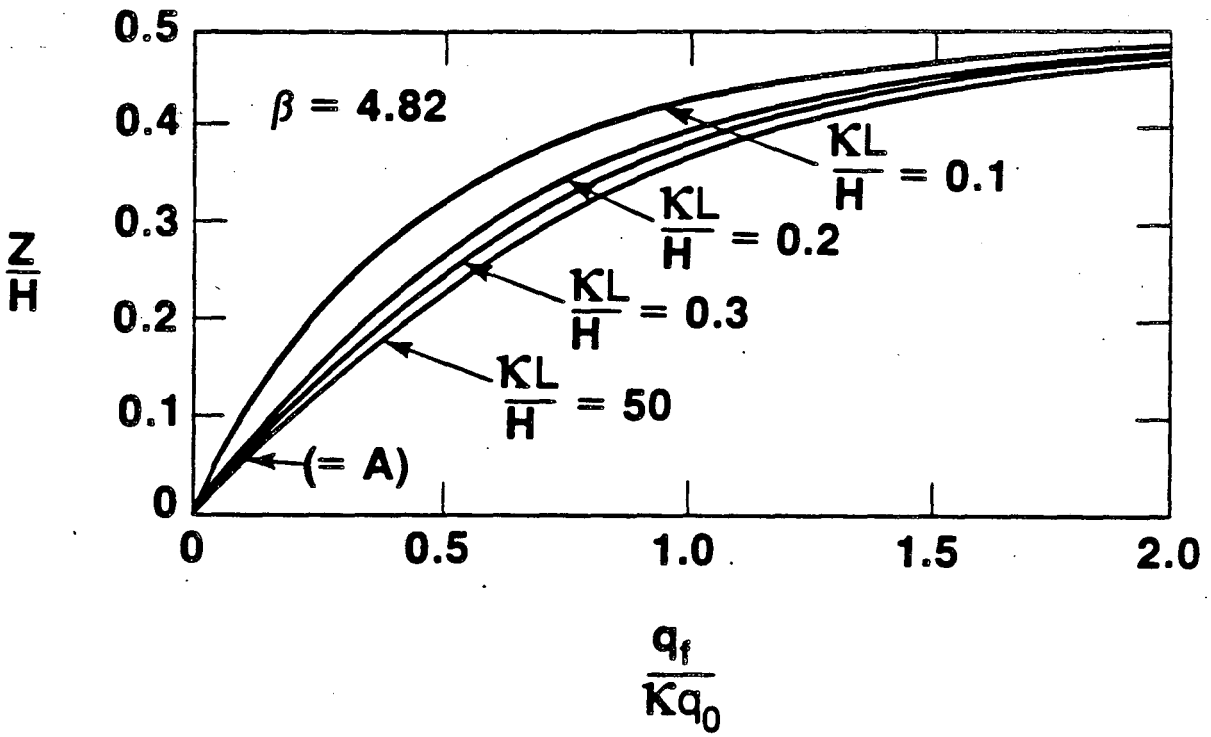

Fig. 5. Dimensionless horizontal groundwater flow across the thermal front for the semi-infinite strip with impermeable left boundary (case B). Variation of the anisotropy factor κ.

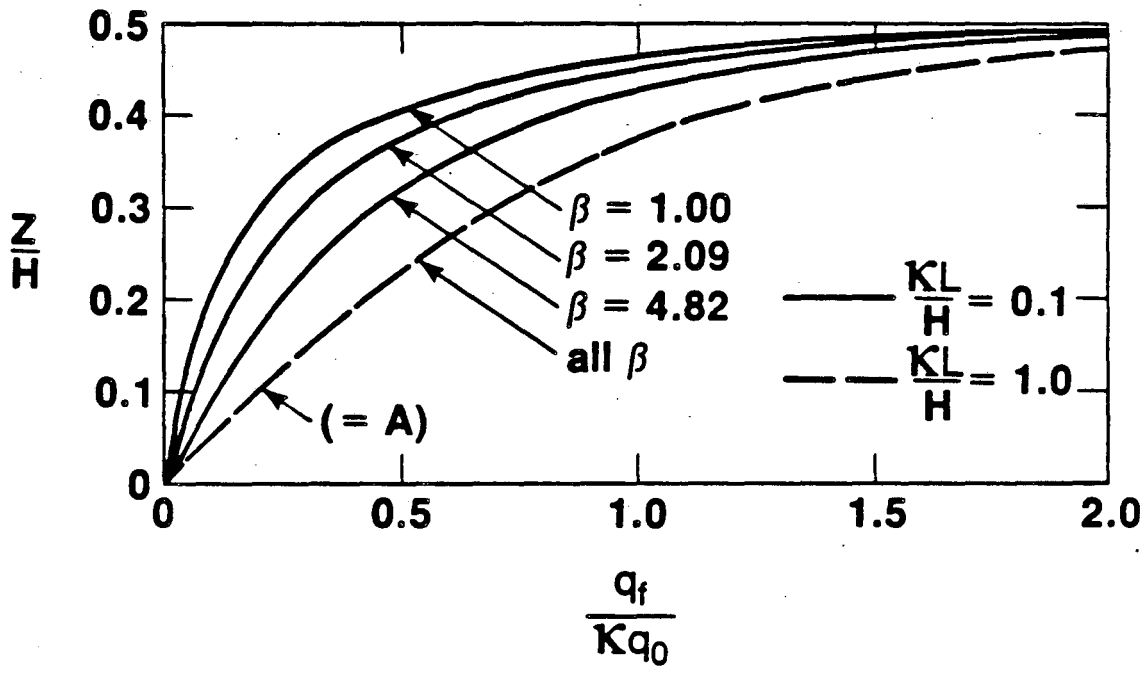

Fig. 6. Dimensionless horizontal groundwater flow across the thermal front for the semi-infinite strip with impermeable left boundary (case B). Variation of the viscosity ratio β.

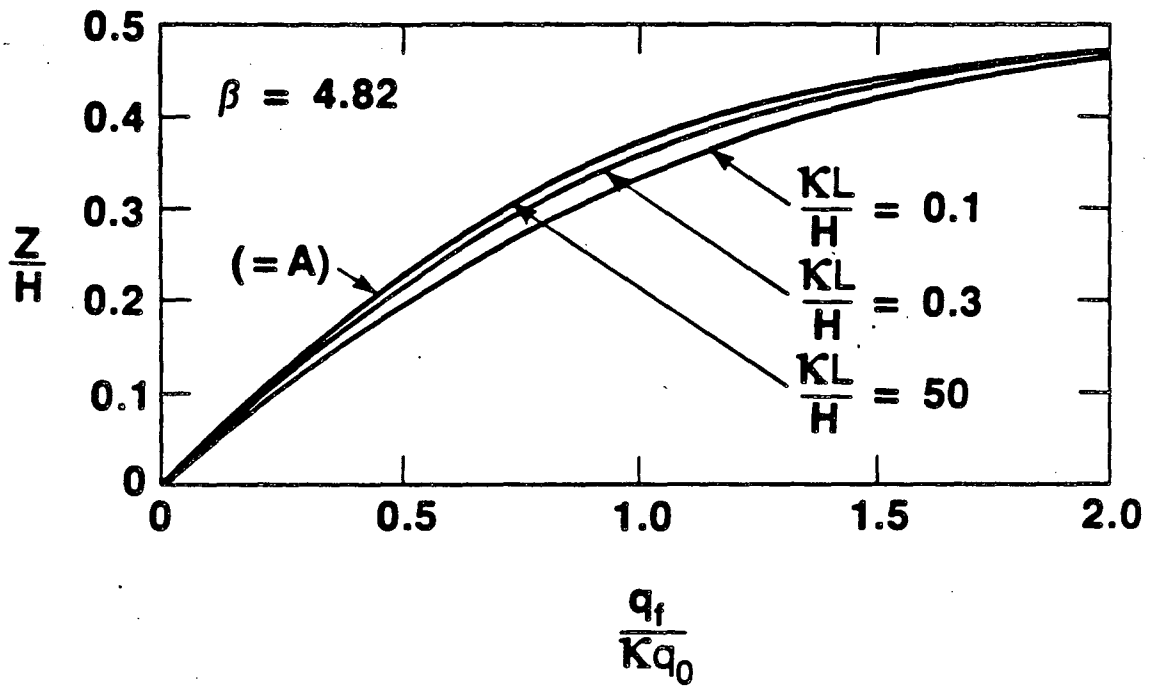

Fig. 7. Dimensionless horizontal groundwater flow across the thermal front for the semi-infinite strip with hydrostatic pressure along the left boundary (case C). Variation of the anisotropy factor κ.

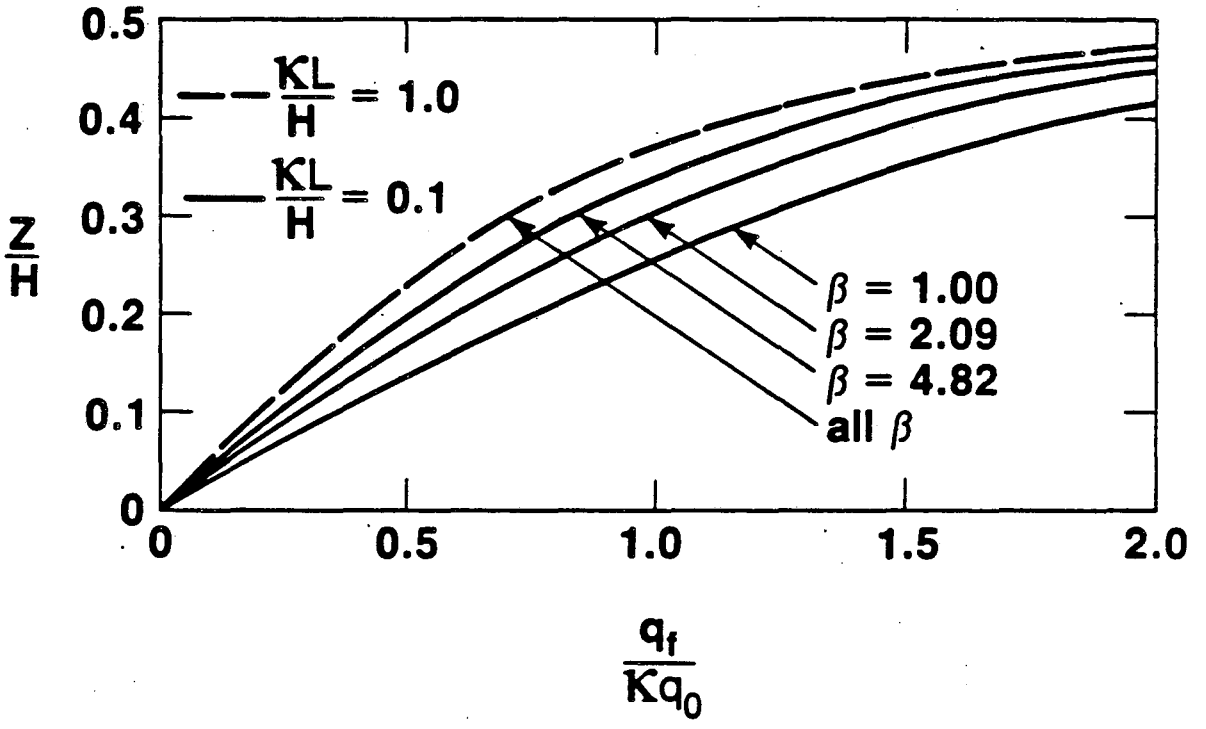

XBL 854-11039

Fig. 8. Dimensionless horizontal groundwater flow across the thermal front for the semi-infinite strip with hydrostatic pressure along the left boundary (case C). Variation of the viscosity ratio β.

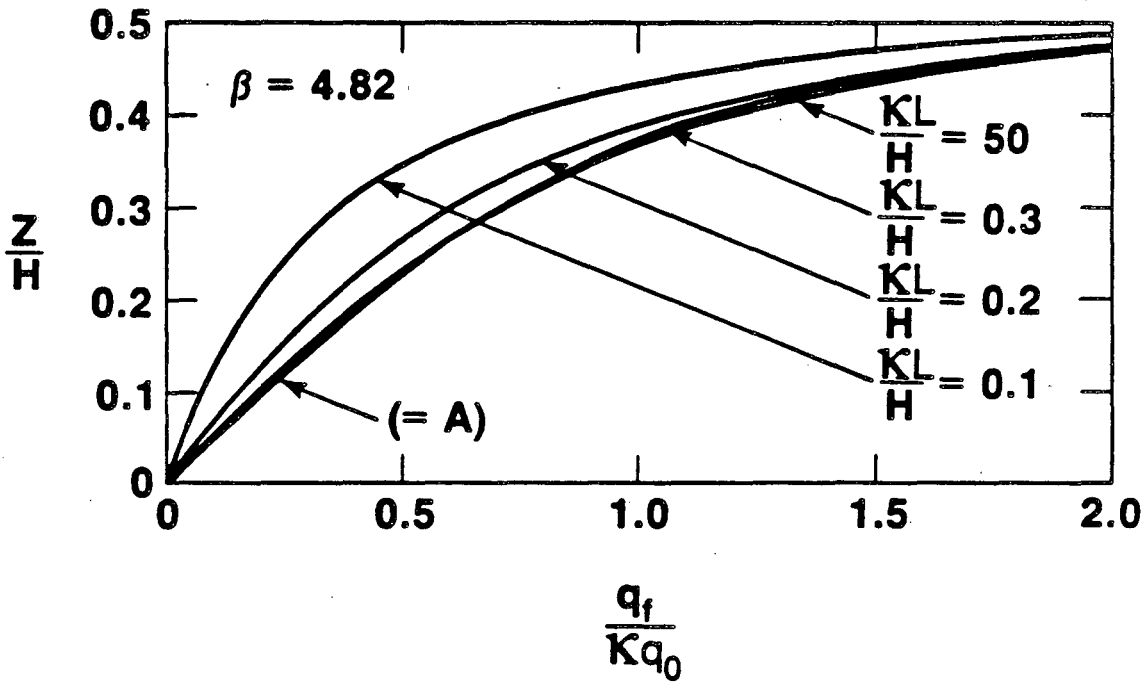

Fig. 9. Dimensionless horizontal groundwater flow across the thermal front for the cylindrical case with no horizontal flow across the inner boundary (case D). Variation of the anisotropy factor κ.

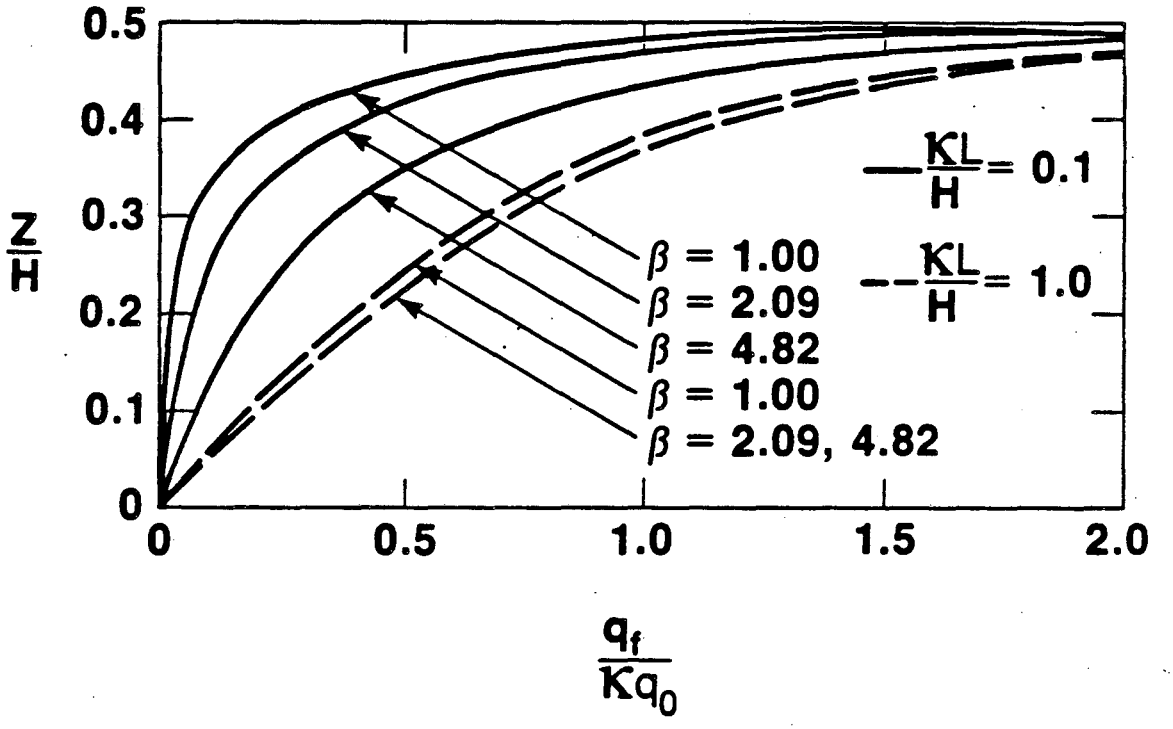

Fig. 10. Dimensionless horizontal groundwater flow across the thermal front for the cylindrical case with no horizontal flow across the inner boundary (case D). Variation of the viscosity ratio β.

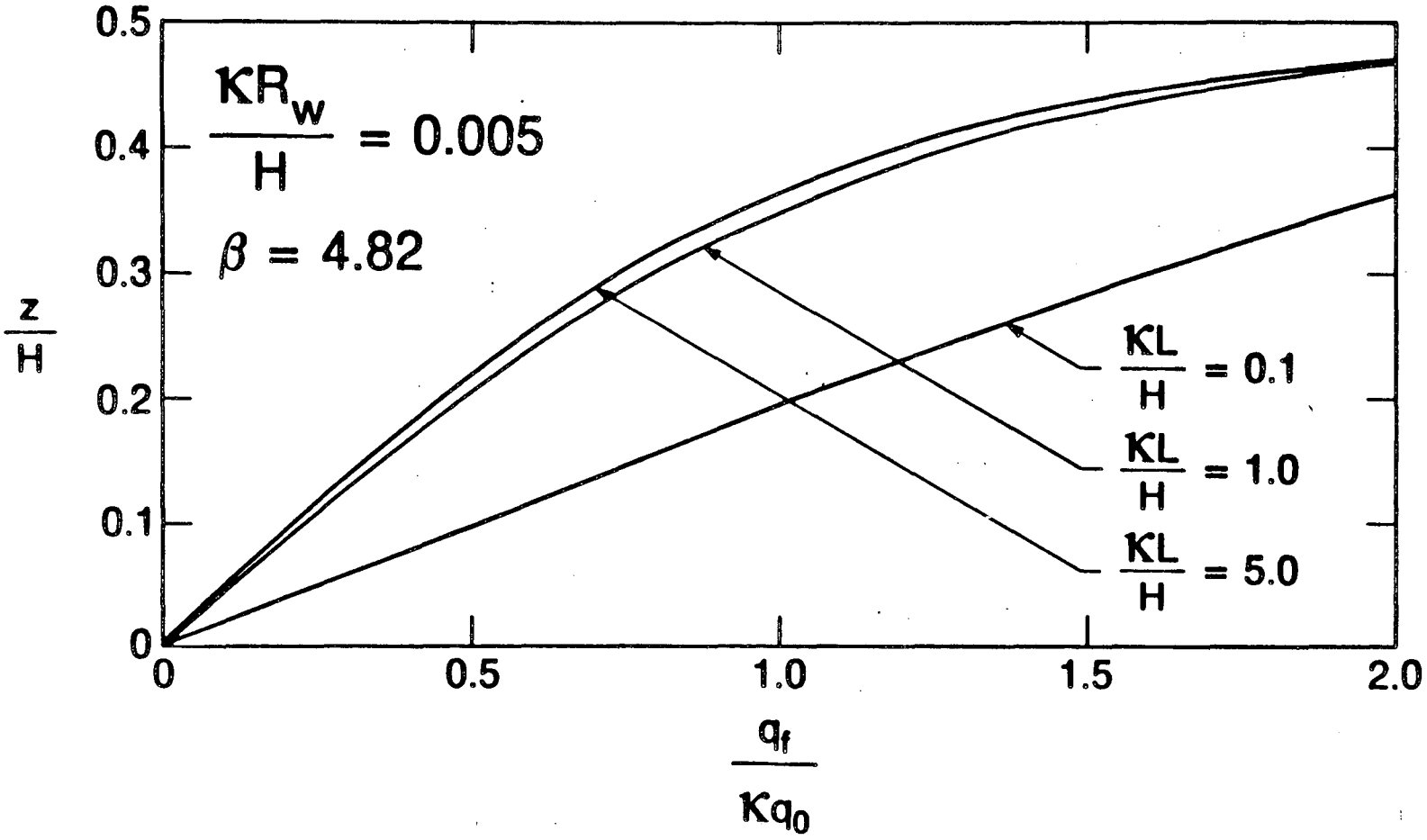

XBL 854-9826

Fig. 11. Dimensionless horizontal groundwater flow across the thermal front for the cylindrical case with hydrostatic pressure conditions at the inner boundary (case E). Variation of the anisotropy factor κ. $\kappa R_w/H = 0.005$.

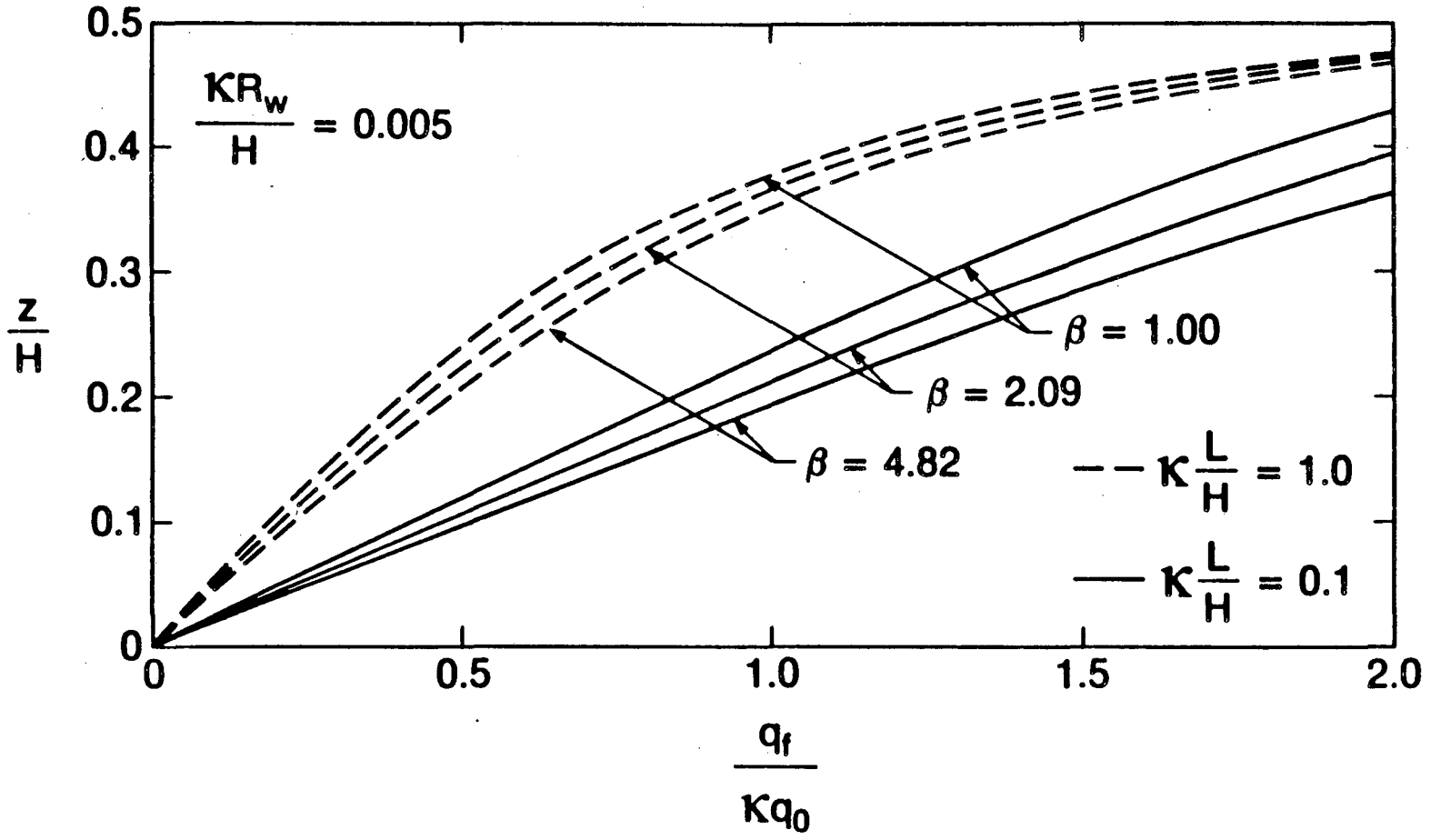

Fig. 12. Dimensionless horizontal groundwater flow across the thermal front for the cylindrical case with hydrostatic pressure conditions at the inner boundary (case E). Variation of the viscosity ratio β. $\kappa R_w / H = 0.005$.

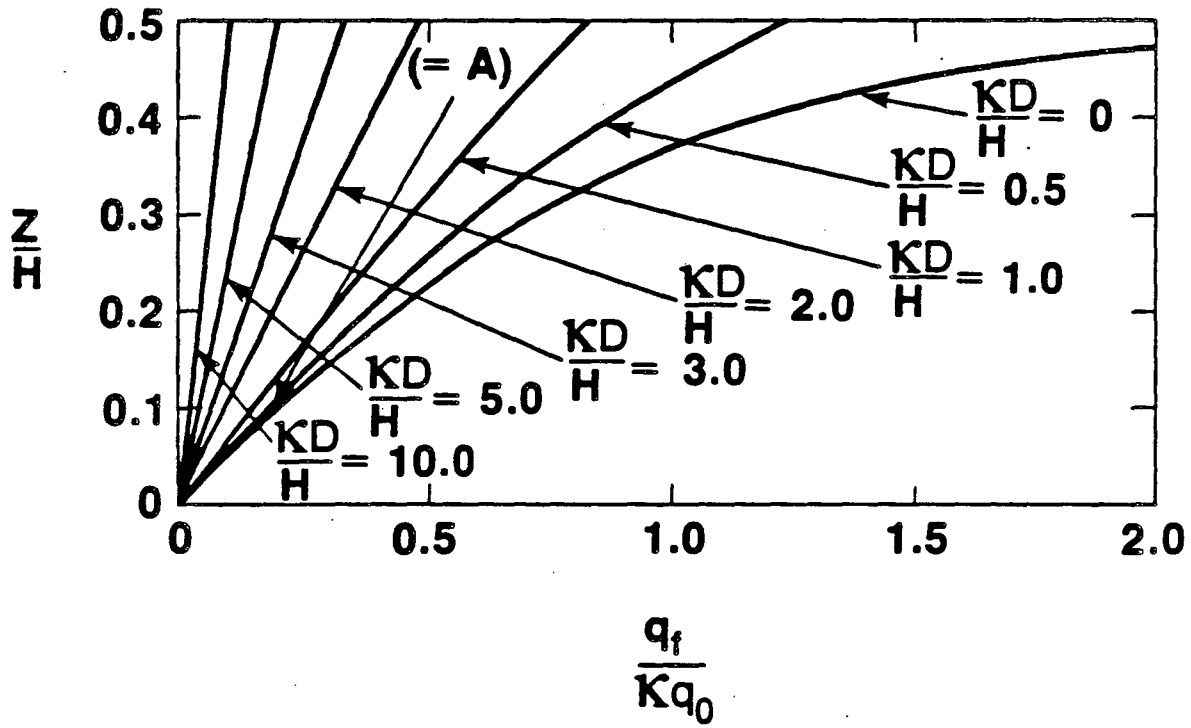

Fig. 13. Dimensionless horizontal groundwater flow across the thermal front for the infinite strip with thermal front thickness D (case F).

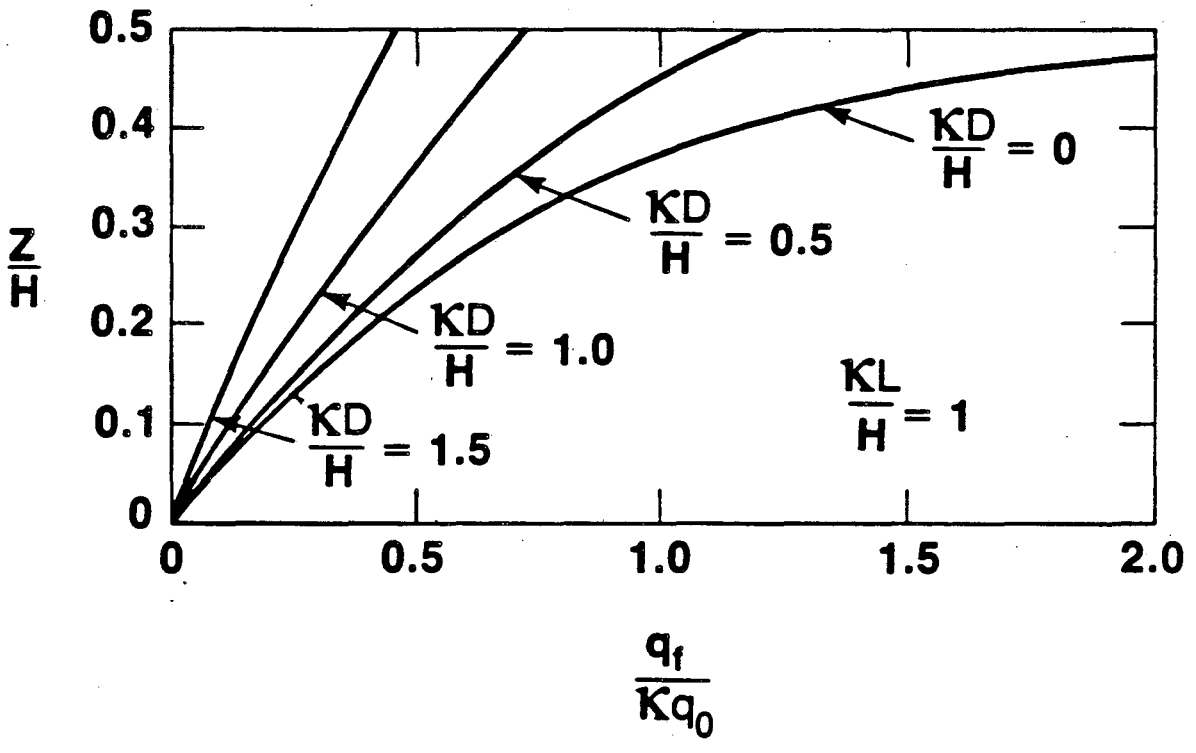

Fig. 14. Dimensionless horizontal groundwater flow across the thermal front for the cylindrical case with thermal front thickness D (case G).

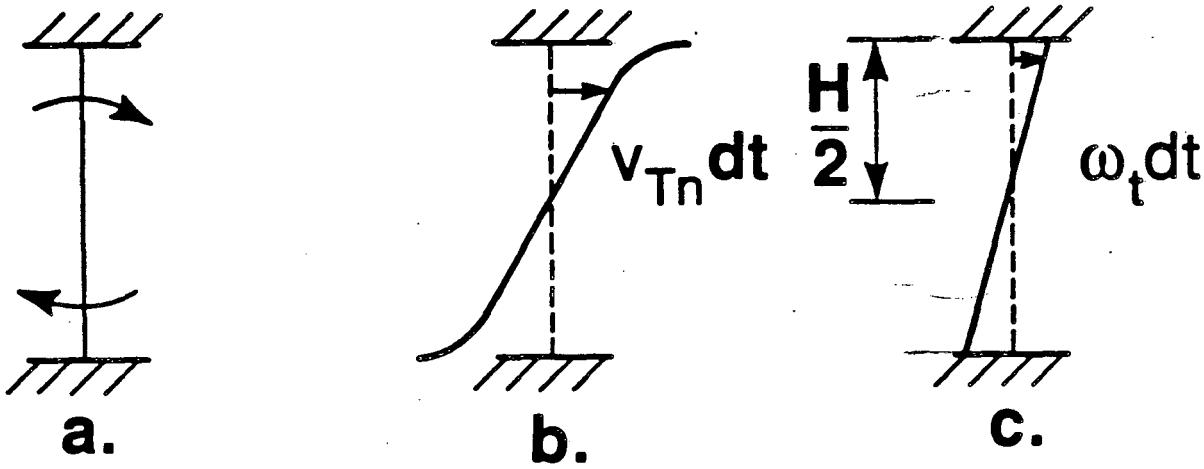

Fig. 15. Definition of the angular tilting rate ω_t. (a) Thermal front at a time t. (b) Thermal front at a time $t+dt$. (c) Linear approximation of situation (b) with the same total flow.

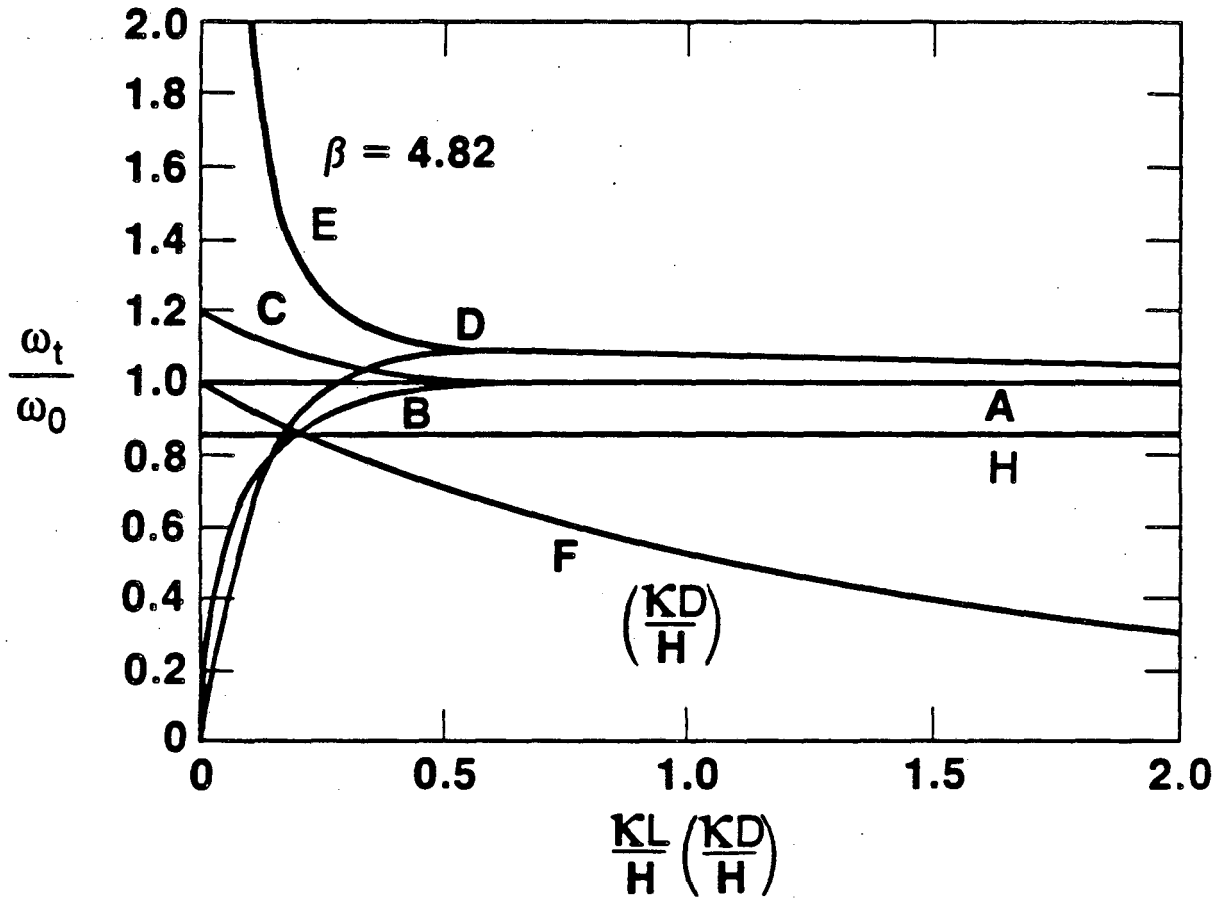

XBL 854-11032

Fig. 16. Tilting rate ω_t for viscosity ratio β=4.82 (T_1=90 ° C, T_0=5 ° C). In case F the tilting rate is given as a function of $\kappa D/H$.

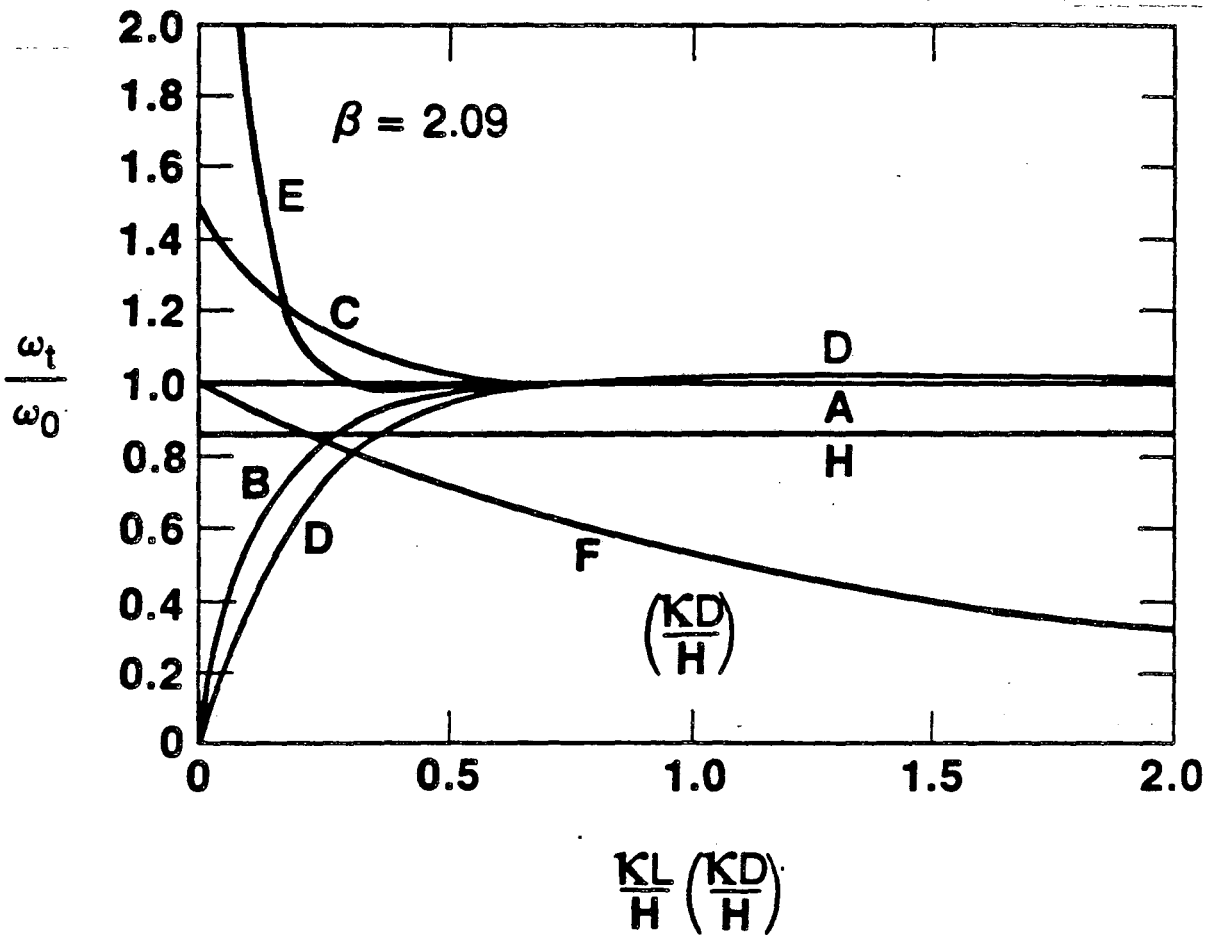

Fig. 17. Tilting rate ω_t for viscosity ratio β=2.09 (T_1=90 °C, T_0=5 °C).

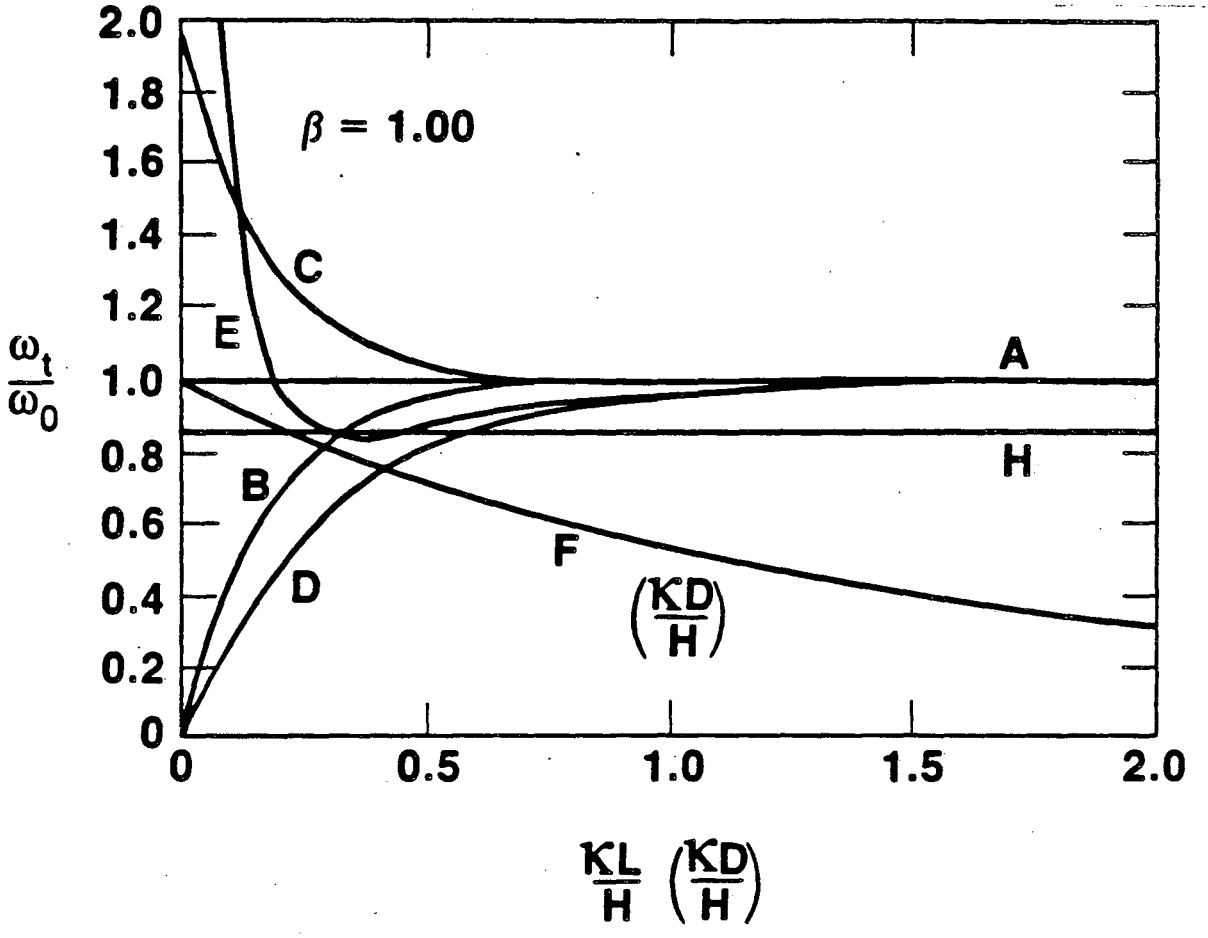

Fig. 18. Tilting rate ω_t for viscosity ratio β=1.

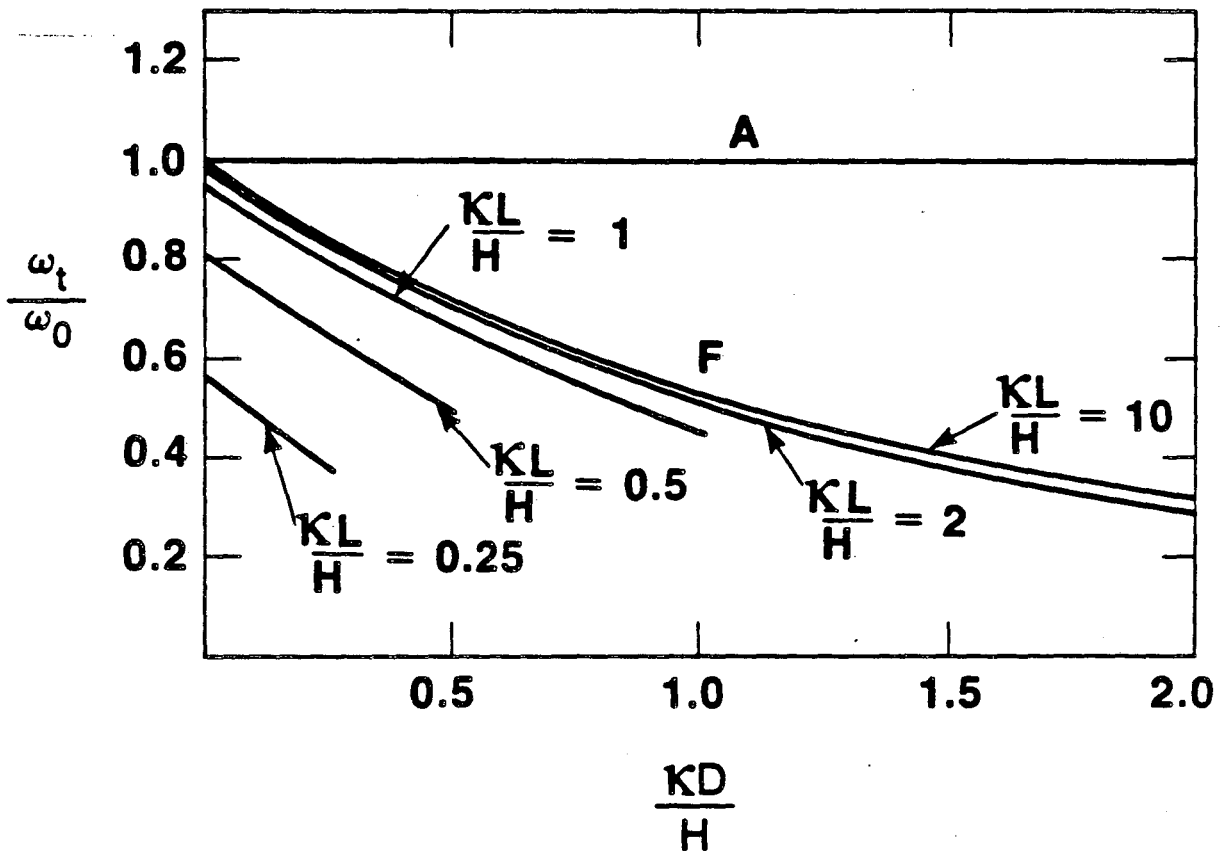

Fig. 19. Tilting rate ω_t for the cylindrical case with thermal front thickness D.

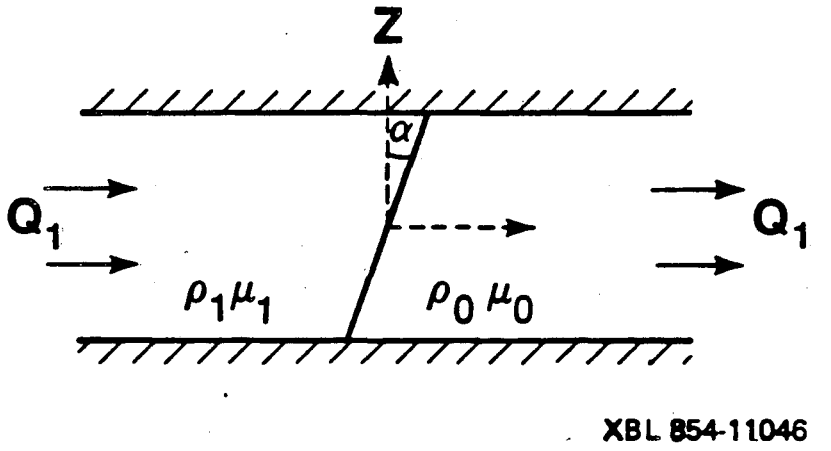

Fig. 20. Aquifer strip with tilted thermal front. Water is pumped through the strip at a flow rate of Q_1.

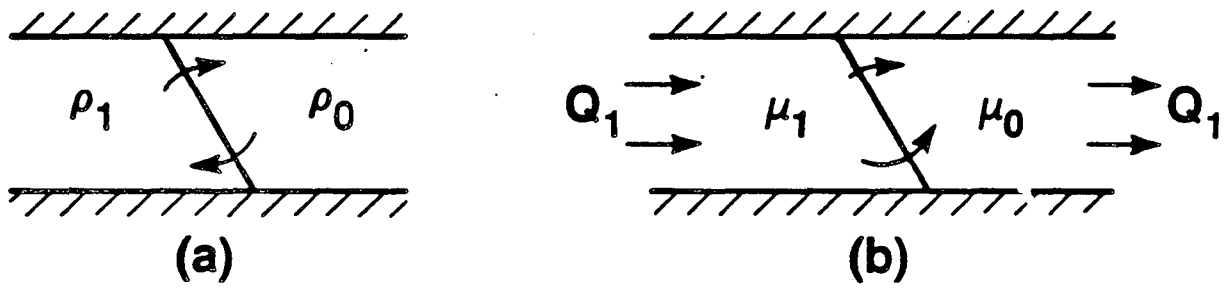

Fig. 21. Aquifer strip with tilted thermal front. (a) Clockwise rotation due to buoyancy flow ($\rho_1 < \rho_0$). (b) Counter-clockwise rotation due to forced convection ($\mu_1 < \mu_0$).

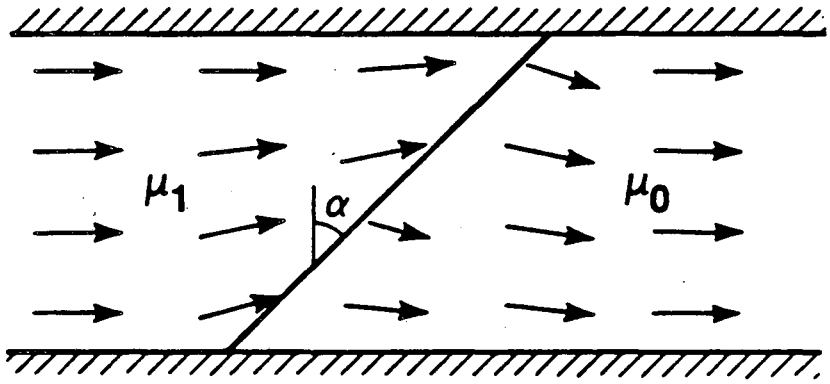

Fig. 22. Groundwater flow pattern for forced convection in an aquifer strip with tilted thermal front.

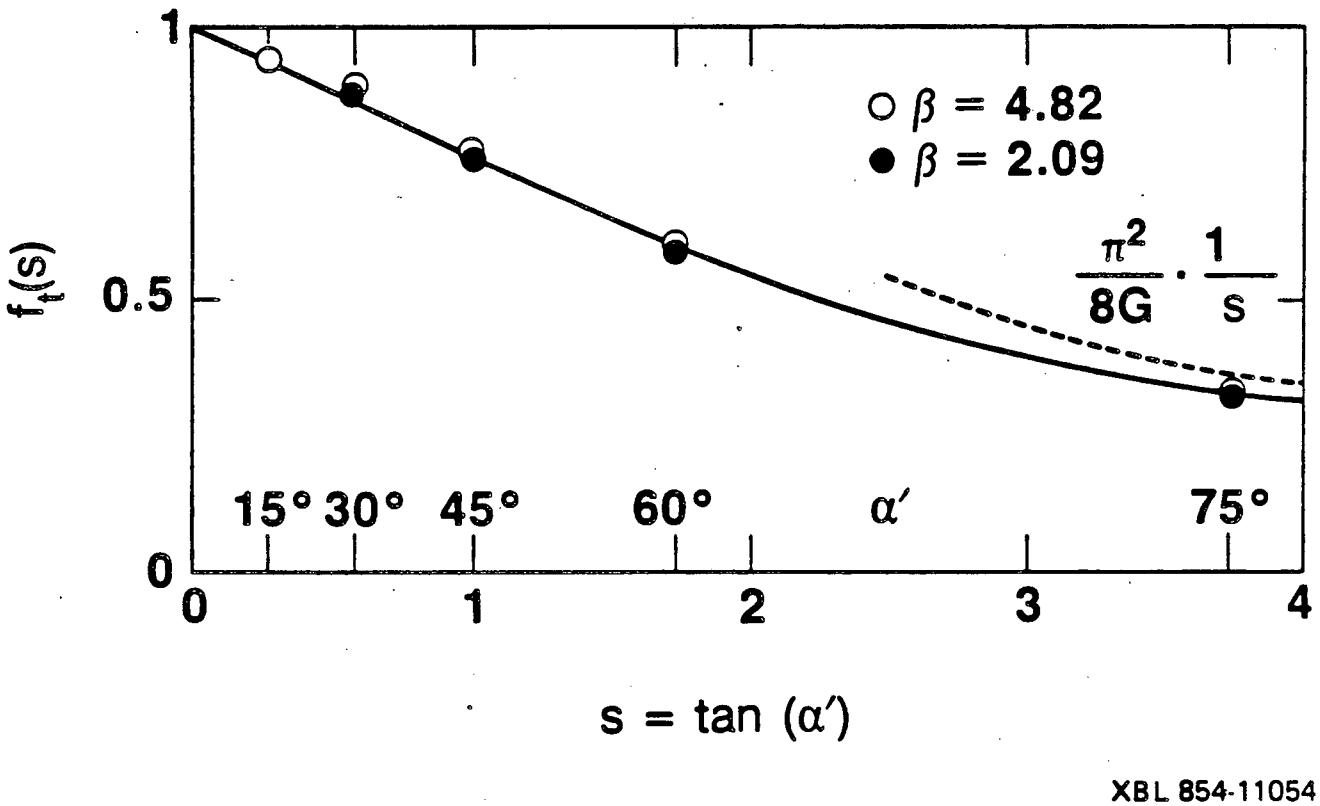

Fig. 23. The quantity (69) as a function of $s = tan\,(\alpha')$. The solid line gives the basic tilting function $f_t(s)$. The dashed line gives the asymptote mentioned in the text.

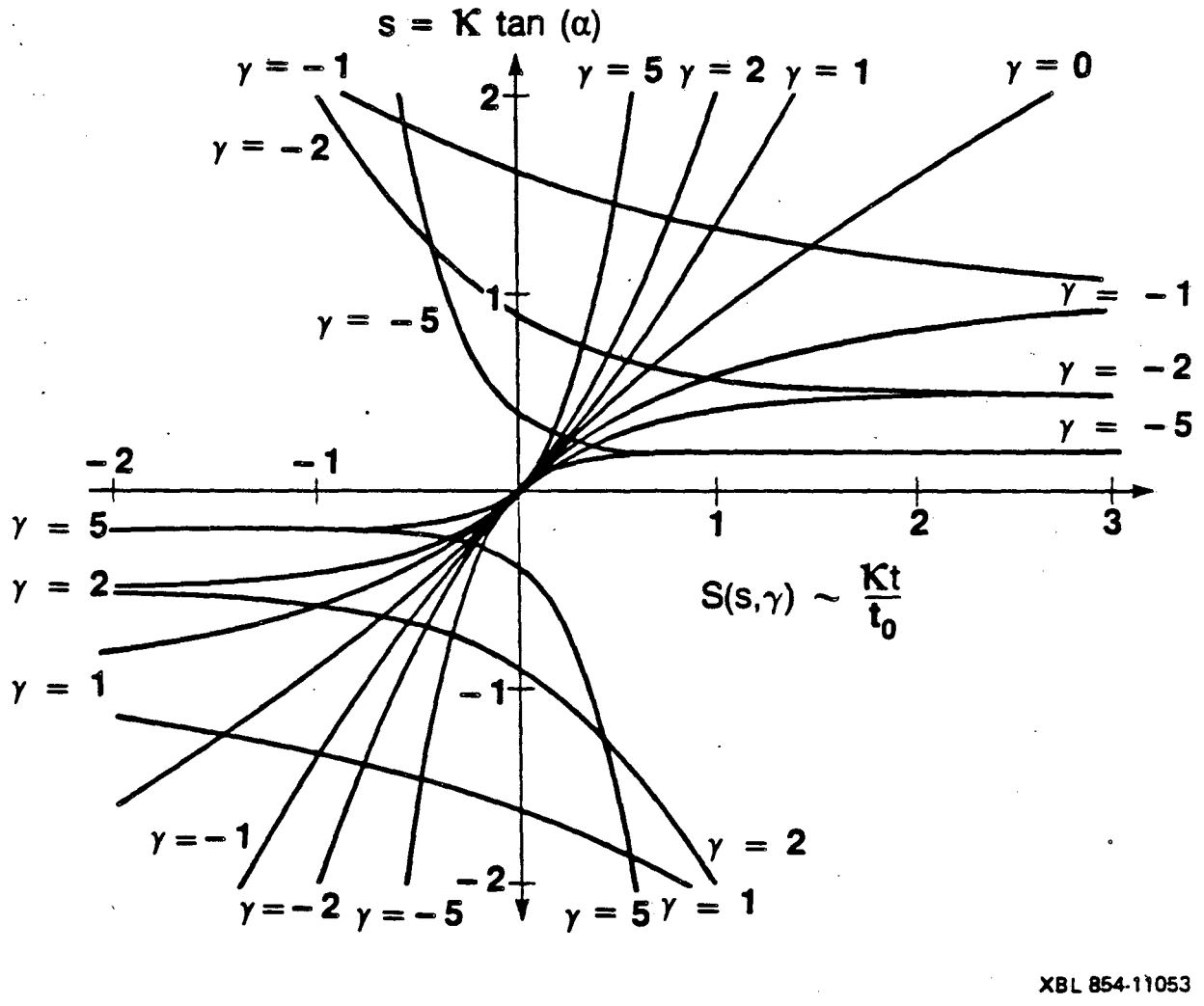

Fig. 24. The function $S(s,\gamma)$. See (83) and (84).

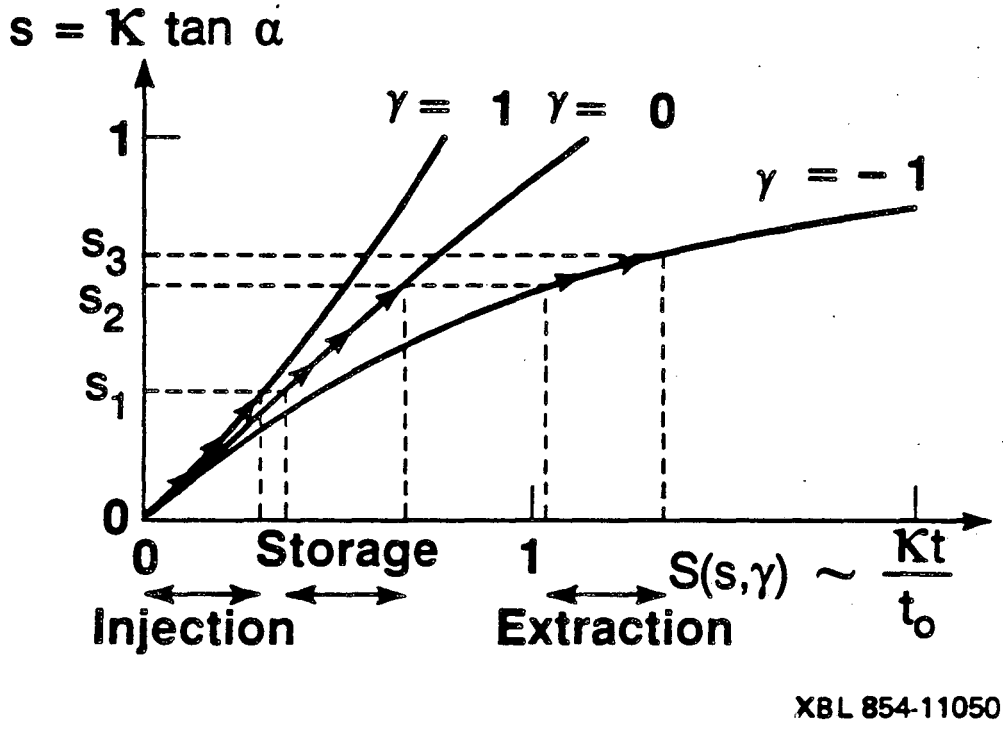

Fig. 25. An example of tilting angle variation $\alpha(t)$ during an injection-storage-extraction cycle.

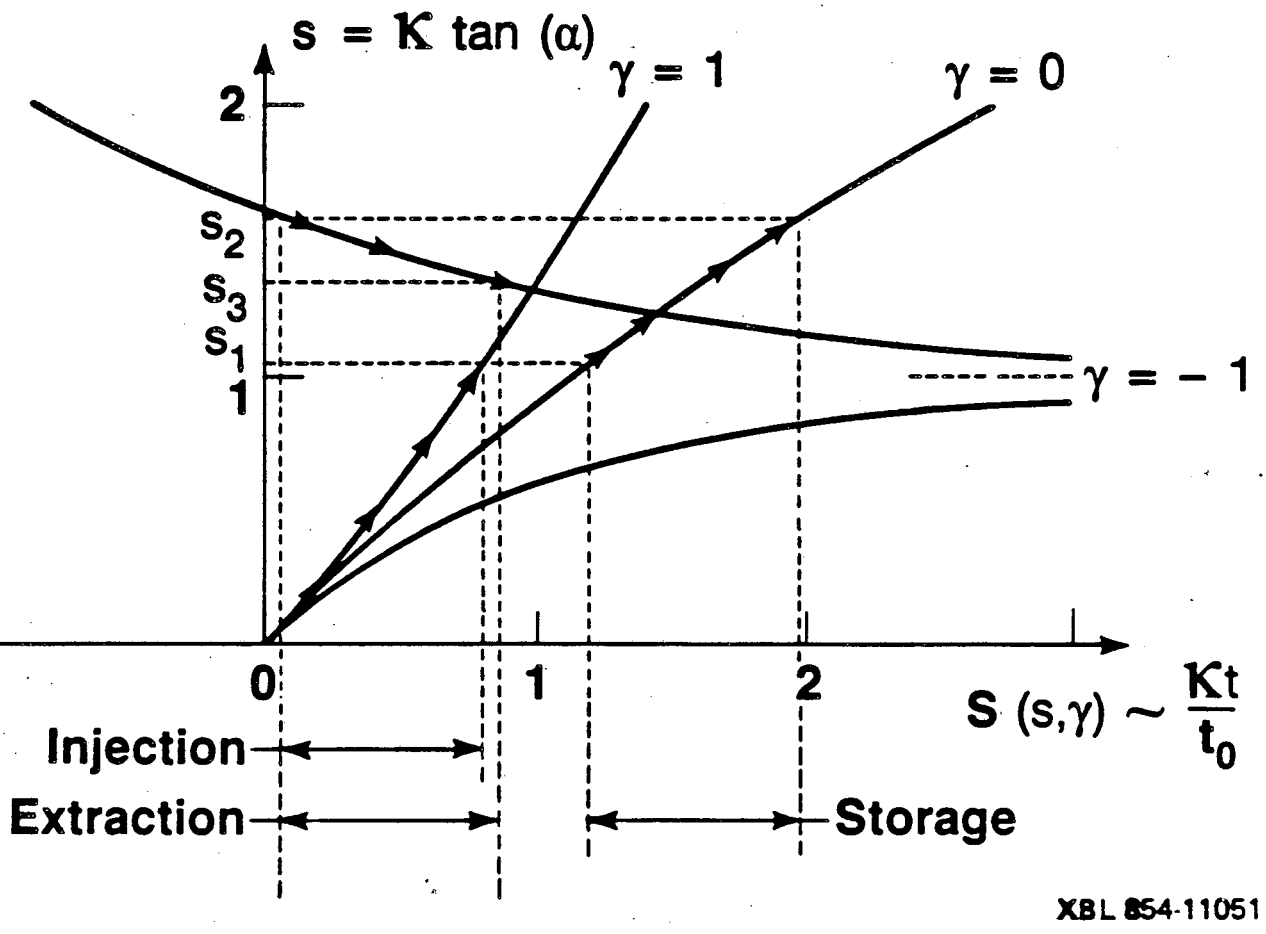

Fig. 26. An example of tilting angle variation $\alpha(t)$ during a longer injection-storage-extraction cycle.

LAWRENCE BERKELEY LABORATORY
TECHNICAL INFORMATION DEPARTMENT
UNIVERSITY OF CALIFORNIA
BERKELEY, CALIFORNIA 94720